Nonperturbative QCD and Quark-Gluon Plasma

Edward V. Shuryak*

Department of Physics and Astronomy, State University of New York, Stony Brook, USA

Lectures given at the
Summer School on Particle Physics
Trieste, 18 June - 6 July 2001

LNS0210002

*shuryak@dau.physics.sunysb.edu

Abstract

This is a brief written version of 5 lectures made at 2001 ICTP Summer School on High Energy Physics in Triest. The lectures provide an overview of what we have learned about QCD vacuum, hadrons and hot/dense hadronic matter during the last 2 decades. Last two lectures contain discussion of heavy ion physics. We focus on the first surprising results from new heavy ion collider, RHIC, as well as recent development toward understanding of the old problem of "soft pomeron" in high energy hadronic collisions and its connection to new heavy ion data.

Contents

1 Introduction

1.1 An outline

In these lectures there are not so many formulae: I tried to clarify the main physics point instead, then jump over years of development to the main questions debated today, and show few recent examples. Systematic discussion of such vast range of subjects need a book[1], not short lecture notes. Technical description of instantons can be found in review [2], and the correlation functions in [4].

We will start in Lecture 1 with the QCD *vacuum structure*, in Lecture 2 we then proceed to the *hadronic structure*, discuss *phases* of hot/dense QCD in Lecture 3, and consider *high energy collisions* of heavy ions and hadrons in lectures 4 and 5, respectively.

The main line in all discussion would be a systematic use of semiclassical methods, specifically the instantons. The reasons for that are: (i) They are the only truly non-perturbative effects understood by now; (ii) They lead to large and probably even dominant effects in many cases; (iii) Due to progress during the last decade, we have near-quantitative theory of instanton effects, solved numerically to *all orders* in the so called 't Hooft interaction.

Although we still do not understand confinement, its companion problem - chiral symmetry breaking in the QCD vacuum - is now understood to a significant degree. Not only we have simple qualitative understanding of where those quasi-zero modes of the Dirac operator come from, but we can calculate their density, space-time shape and eventually **QCD correlation functions** with surprising accuracy. So, in a way, the problem of hadronic structure is nearly solved for light-quark hadrons[2].

As we will see below, although the high density and temperature domain can be understood in the (re-summed) perturbation theory, the boundaries of the QCD phases is a matter of non-perturbative physics. I will argue that this phase diagram can also be understood based on the instanton framework. The of three basic phases of QCD: (i) hadronic phase, (ii) Quark-Gluon Plasma (QGP) and (iii) Color Superconductor (CS) phases appear as a balance between three basic pairing channels, being (i) attraction in scalar colorless $\bar{q}q$ channel; (ii) instanton-antiinstanton pairing induced by light quark exchanges; and (iii) attraction in scalar but colored qq channels.

[1] I wrote such a book in mid-80's, [1], and now am working at its new edition.

[2] Medium-heavy-quark ones, such as $\bar{c}c, \bar{b}b$ do care about confining potential, while (hypothetical) extremely heavy quarkonia would need only the Coulomb forces.

The last part deals with high energy collisions of hadrons and heavy ions: those are related to the rest of the lectures since this is how we try to access another QCD phase, the Quark-Gluon Plasma, experimentally. We will discuss first results coming from RHIC, show that matter produced seems to behave macroscopically (namely, hydrodynamically) with proper Equation of State. We will also try to connect rapid onset of QGP equilibration with existing ideas based on perturbative and non-perturbative mechanisms. We will argue that tunneling dynamics described by instantons not only play role in vacuum, but in collisions as well. In this case, however, quantum paths describing the process can transfer from Euclidean to Minkowski space, crossing the so called "turning states" on the way. A sphaleron known in electroweak theory is one of them, and we will argue that those states are physically produced in high energy collisions.

1.2 Scales of QCD

Let me start with an introductory discussion of various "scales" of non-perturbative QCD. The major reason I do this is the following: some naive simplistic ideas we had in the early days of QCD, in the 70's, are still alive today. I would strongly argue against the picture of non-perturbative objects as some structure-less fields with typical momenta of the order of $p \sim \Lambda_{QCD} \sim (1\,fm)^{-1}$. In the mid-70's people considered hadrons to be structure-less "bags" filled with near-massless perturbative quarks, with mild non-perturbative effects appearing at its boundaries and confining them at the scale of 1 fm.

One logical consequence of this picture would be applicability of the derivative expansion of the non-perturbative fields or Operator Product Expansion (OPE), the basis of the QCD sum rules. However, after the first successful applications of the method [5] rather serious problems[7] have surfaced. All spin-zero channels (as we will see, those are the ones directly coupled to instantons) related with quark or gluon-based operators alike, indicate unexpectedly large non-perturbative effects and deviate from the OPE predictions at very small distances.

It provided a very important lesson: *the non-perturbative fields form structures with sizes significantly smaller than 1 fm* and local field strength much larger than Λ^2. Instantons are one of them: in order to describe many of these phenomena in a consistent way one needs instantons of small size [6] $\rho \sim 1/3\,fm$. We have direct confirmation of it from the lattice, but not

real understanding of why there are no large-size instantons.

Furthermore, the instanton is not the only such small-scale gluonic object. We also learned from the lattice-based works that QCD flux tubes (or confining strings) also have small radius, only about $r_{string} \approx 1/5\, fm$. So, all hadrons (and clearly the QCD vacuum itself) have a *substructure*, with "constituent quarks" generated by instantons connected by such flux tubes.

Clearly this substructure should play an important role in hadronic physics. We would like to know why the usual quark model has been so successful in spectroscopy, and why so little of exotic states have been seen. Also, high energy hadronic collisions must tell us a lot about substructure, since the famous Pomeron also belongs to a list of those surprisingly small non-perturbative objects.

At the opposite end of the spectrum, people have found that QCD seem to have also surprisingly *small energy/momentum scale*, several times lower than Λ. It was found that behavior of the so called "quenched" and true QCD is very different, but only if the quark mass is below some scale of the order of 20-50 MeV. As we will see below, this surprising low scale has been explained by properties of the instanton ensemble.

2 Lecture 1. The QCD vacuum

2.1 Chiral symmetry breaking and instantons

Let me start around 1961, when the ideas about chiral symmetry and what it may take to break it spontaneously have appeared. The NJL model [13] was the first microscopic model which attempted to derive dynamically the properties of chiral symmetry breaking and pions, starting from some *hypothetical 4-fermion interaction.*

$$L_{NJL} = G(\vec{\pi}^2 + \sigma^2) \tag{1}$$

where π, σ denote the corresponding scalar isovector and scalar isoscalar currents.

Let me make few comments about it.

(i) It was the first bridge between the BCS theory of superconductivity and quantum field theory, leading the way to the Standard Model. It first showed that the vacuum can be truly nontrivial, a superconductor of a kind, with the mass gap Δ=330-400 MeV, known as "constituent quark mass".

(ii) The NJL model has 2 parameters: the strength of its 4-fermion interaction G and the cutoff $\Lambda \sim .8 - 1 GeV$. The latter regulates the loops (the model is non-renormalizable, which is OK for an effective theory) and is directly the "chiral scale" we are discussing. We will relate Λ to the typical instanton size ρ, and G to a combination $n\rho^2$ of the size and density of instantons.
(iii) One non-trivial prediction of the NJL model was a the mass of the scalar is $m_\sigma \approx 2m_{const.quark}$. Because this state is the P-wave in non-relativistic language, it means that there is strong attraction which is able to compensate exactly for rotational kinetic energy. For decades simpler hadronic models failed to get this effect, and even now spectroscopists still argue that this (40-year-old!) result is incorrect. However, lattice results in fact show that it is exactly right and theoretically understood by instantons. Moreover, the phenomenological sigma meson is being revived now, so possibly it will even get back to its proper place in Particle Data Table, after decades of absence.

Let me now jump to instantons. We will show below that they generate quite specific 4-fermion 't Hooft interaction [12] (for 2-flavor theory: for pedagogical reasons we ignore strange quarks altogether now). Furthermore, its Lagrangian includes the NJL one, but it also has 2 new terms:

$$L_{tHooft} = G(\vec{\pi}^2 + \sigma^2 - \eta^2 - \vec{\delta}^2) \tag{2}$$

with isoscalar pseudoscalar η and isovector scalar $\vec{\delta}$. T'Hooft's minus sign is crucial here: it shows that the axial U(1) symmetry (e.g. rotation of sigma into eta) is *not* a symmetry. That is why η (actuallyη' if strangeness is included) is *not* massless Goldstone particle like a pion.

The most important next development happened in 1980's: it has been shown in [6, 14] that instanton-induced interaction does break *spontaneously* the $SU(N_f)$ chiral symmetry. Unlike the NJL model, the instanton-induced interaction has a natural cut-off parameter ρ, and the coupling constants are not free parameters, but determined by a physical quantity, the instanton density. That eventually allowed to solve in all orders in 't Hooft interaction, and get quantitative results, see [2].

2.2 General things about the instantons

I would omit from this paper general things about the instantons, well covered elsewhere. Let me just briefly mention that the topologically-nontrivial

4d solution was found by Polyakov and collaborators in[8], and soon it was interpreted as semi-classical tunneling between topologically non-equivalent vacua. The name itself was suggested by t Hooft, meaning "existing for an instant". Formally, instantons appear in the context of the semi-classical approximation to the (Euclidean) QCD partition function

$$Z = \int DA_\mu \, \exp(-S) \prod_f^{N_f} \det\left(\not{D} + m_f\right), \tag{3}$$

$$S = \frac{1}{4g^2} \int d^4x \, G^a_{\mu\nu} G^a_{\mu\nu}. \tag{4}$$

Here, S is the gauge field action and the determinant of the Dirac operator $\not{D} = \gamma_\mu(\partial_\mu - iA_\mu)$ accounts for the contribution of fermions. In the semi-classical approximation, we look for saddle points of the functional integral (3), i.e. configurations that minimize the classical action S. This means that saddle point configurations are solutions of the classical equations of motion.

These solutions can be found using the identity

$$S = \frac{1}{4g^2} \int d^4x \, \left[\pm G^a_{\mu\nu} \tilde{G}^a_{\mu\nu} + \frac{1}{2} \left(G^a_{\mu\nu} \mp \tilde{G}^a_{\mu\nu} \right)^2 \right], \tag{5}$$

where $\tilde{G}_{\mu\nu} = 1/2 \epsilon_{\mu\nu\rho\sigma} G_{\rho\sigma}$ is the dual field strength tensor (the field strength tensor in which the roles of electric and magnetic fields are reversed). Since the first term is a topological invariant (see below) and the last term is always positive, it is clear that the action is minimal if the field is (anti) self-dual

$$G^a_{\mu\nu} = \pm \tilde{G}^a_{\mu\nu}. \tag{6}$$

The action of a self-dual field configuration is determined by its topological charge

$$Q = \frac{1}{32\pi^2} \int d^4x \, G^a_{\mu\nu} \tilde{G}^a_{\mu\nu}. \tag{7}$$

From (5), we have $S = (8\pi^2|Q|)/g^2$. For finite action configurations, Q has to be an integer. The instanton is a solution with $Q = 1$ [8]

$$A^a_\mu(x) = \frac{2\eta_{a\mu\nu} x_\nu}{x^2 + \rho^2}, \tag{8}$$

where the 't Hooft symbol $\eta_{a\mu\nu}$ is defined by

$$\eta_{a\mu\nu} = \begin{cases} \epsilon_{a\mu\nu} & \mu, \nu = 1, 2, 3, \\ & \delta_{a\mu}\nu = 4, \\ & -\delta_{a\nu}\mu = 4. \end{cases} \tag{9}$$

and ρ is an arbitrary parameter characterizing the size of the instanton. This original instanton has its non-trivial topology at large distances, but if we are to consider instanton ensemble, its another form, the so called *singular gauge* on is needed

$$A^a_\mu(x) = \frac{2\bar{\eta}_{a\mu\nu} x_\nu \rho^2}{(x^2+\rho^2)x^2}, \tag{10}$$

because in this case the non-trivial topology is at the point singularity.

The classical instanton solution has a number of degrees of freedom, known as collective coordinates. In addition to the size, the solution is characterized by the instanton position z_μ and the color orientation matrix R^{ab} (corresponding to color rotations $A^a_\mu \to R^{ab}A^b_\mu$). A solution with topological charge $Q=-1$ can be constructed by replacing $\eta_{a\mu\nu} \to \overline{\eta}_{a\mu\nu}$, where $\overline{\eta}_{a\mu\nu}$ is defined by changing the sign of the last two equations in (9).

The physical meaning of the instanton solution becomes clear if we consider the classical Yang-Mills Hamiltonian (in the temporal gauge, $A_0=0$)

$$H = \frac{1}{2g^2}\int d^3x\,(E_i^2+B_i^2), \tag{11}$$

where E_i^2 is the kinetic and B_i^2 the potential energy term. The classical vacua corresponds to configurations with zero field strength. For non-abelian gauge fields this limits the gauge fields to be "pure gauge" $A_i = iU(\vec{x})\partial_i U(\vec{x})^\dagger$. Such configurations are characterized by a topological winding number n_W which distinguishes between gauge transformations U that are not continuously connected.

This means that there is an infinite set of classical vacua enumerated by an integer n. Instantons are tunneling solutions that connect the different vacua. They have potential energy $B^2>0$ and kinetic energy $E^2<0$, their sum being zero at any moment in time. Since the instanton action is finite, the barrier between the topological vacua can be penetrated, and the true vacuum is a linear combination $|\theta\rangle = \sum_n e^{in\theta}|n\rangle$ called the theta vacuum. In QCD, the value of θ is an external parameter. If $\theta \neq 0$ the QCD vacuum breaks CP invariance. Experimental limits on CP violation require[3] $\theta < 10^{-9}$.

[3]The question why θ happens to be so small is known as the "strong CP problem". Most likely, the resolution of the strong CP problem requires physics outside QCD and we will not discuss it any further.

The rate of tunneling between different topological vacua is determined by the semi-classical (WKB) method. From the single instanton action one expects

$$P_{tunneling} \sim \exp(-8\pi^2/g^2). \tag{12}$$

The factor in front of the exponent can be determined by taking into account fluctuations $A_\mu = A_\mu^{cl} + \delta A_\mu$ around the classical instanton solution. This calculation was performed in a classic paper by 't Hooft [12]. The result is

$$dn_I = \frac{0.47\exp(-1.68N_c)}{(N_c-1)!(N_c-2)!}\left(\frac{8\pi^2}{g^2}\right)^{2N_c}\exp\left(-\frac{8\pi^2}{g^2(\rho)}\right)\frac{d^4z d\rho}{\rho^5}, \tag{13}$$

where $g^2(\rho)$ is the running coupling constant at the scale of the instanton size. Taking into account quantum fluctuations, the effective action depends on the instanton size. This is a sign of the conformal (scale) anomaly in QCD. Using the one-loop beta function the result can be written as $dn_I/(d^4z) \sim d\rho\rho^{-5}(\rho\Lambda)^b$ where $b = (11N_c/3) = 11$ is the first coefficient of the beta function. Since b is a large number, small size instantons are strongly suppressed. On the other hand, there appears to be a divergence at large ρ. In this regime, however, the perturbative analysis based on the one loop beta function is not applicable.

2.3 *Zero Modes and the $U(1)_A$ anomaly*

In the last section we showed that instantons interpolate between different topological vacua in QCD. It is then natural to ask if the different vacua can be physically distinguished. This question is answered most easily in the presence of light fermions, because the different vacua have different axial charge. This observation is the key element in understanding the mechanism of chiral anomalies.

Anomalies first appeared in the context of perturbation theory [9, 10]. From the triangle diagram involving an external axial vector current one finds that the flavor singlet current which is conserved on the classical level develops an anomalous divergence on the quantum level

$$\partial_\mu j_\mu^5 = \frac{N_f}{16\pi^2}G_{\mu\nu}^a\tilde{G}_{\mu\nu}^a. \tag{14}$$

This anomaly plays an important role in QCD, because it explains the absence of a ninth goldstone boson, the so called $U(1)_A$ puzzle.

The mechanism of the anomaly is intimately connected with instantons. First, we recognize the integral of the RHS of (14) as $2N_f Q$, where Q is the topological charge. This means that in the background field of an instanton we expect axial charge conservation to be violated by $2N_f$ units. The crucial property of instantons, originally discovered by 't Hooft, is that the Dirac operator has a zero mode $i\not{D}\psi_0(x) = 0$ in the instanton field. For an instanton in the singular gauge, the zero mode wave function is

$$\psi_0(x) = \frac{\rho}{\pi}\frac{1}{(x^2+\rho^2)^{3/2}}\frac{\gamma\cdot x}{\sqrt{x^2}}\frac{1+\gamma_5}{2}\phi \tag{15}$$

where $\phi^{\alpha m} = \epsilon^{\alpha m}/\sqrt{2}$ is a constant spinor, which couples the color index α to the spin index $m = 1, 2$. Note that the solution is left handed, $\gamma_5\psi_0 = -\psi_0$. Analogously, in the field of an anti-instanton there is a right handed zero mode.

We can now see how axial charge is violated during tunneling. For this purpose, let us consider the Dirac Hamiltonian $i\vec{\alpha}\cdot\vec{D}$ in the field of the instanton. The presence of a 4-dimensional normalizable zero mode implies that there is one left handed state that crosses from positive to negative energy during the tunneling event. This can be seen as follows: In the adiabatic approximation, solutions of the Dirac equation are given by

$$\psi_i(\vec{x},t) = \psi_i(\vec{x},t=-\infty)\exp\left(-\int_{-\infty}^{t} dt'\,\epsilon(t')\right). \tag{16}$$

The only way we can have a 4-dimensional normalizable wave function is if ϵ_i is positive for $t\to\infty$ and negative for $t\to-\infty$. This explains how axial charge can be violated during tunneling. No fermion ever changes its chirality, all states simply move one level up or down. The axial charge comes, so to say, from the "bottom of the Dirac sea".

2.4 *The effective interaction between quarks*

Proceeding from pure glue theory to QCD with light quarks, one has to deal with the much more complicated problem of quark-induced interactions. Indeed, on the level of a single instanton we can not even understand the presence of instantons in full QCD. The reason is again related to the existence of zero modes. In the presence of light quarks, the tunneling rate is proportional to the fermion determinant, which is given by the product of the eigenvalues of the Dirac operator. This means that (as $m\to 0$) the tunneling amplitude vanishes and individual instantons cannot exist!

This result is related to the anomaly: During the tunneling event, the axial charge of the vacuum changes, so instantons have to be accompanied by fermions. The tunneling amplitude is non-zero only in the presence of external quark sources, because zero modes in the denominator of the quark propagator can cancel against zero modes in the determinant. Consider the fermion propagator in the instanton field

$$S(x,y) = \frac{\psi_0(x)\psi_0^+(y)}{im} + \sum_{\lambda\neq 0} \frac{\psi_\lambda(x)\psi_\lambda^+(y)}{\lambda + im} \tag{17}$$

where $i\not{D}\psi_\lambda = \lambda\psi_\lambda$. For N_f light quark flavors the instanton amplitude is proportional to m^{N_f}. Instead of the tunneling amplitude, let us calculate a $2N_f$-quark Green's function $\langle \prod_f \bar{\psi}_f(x_f)\Gamma\psi_f(y_f)\rangle$, containing one quark and antiquark of each flavor. Performing the contractions, the amplitude involves N_f fermion propagators (17), so that the zero mode contribution involves a factor m^{N_f} in the denominator.

The result can be written in terms of an effective Lagrangian [12]. It is a non-local $2N_f$-fermion interaction, where the quarks are emitted or absorbed in zero mode wave functions. The result simplifies if we take the long wavelength limit (in reality, the interaction is cut off at momenta $k > \rho^{-1}$) and average over the instanton position and color orientation. For $N_f = 1$ the result is [12, 15]

$$\mathcal{L}_{N_f=1} = \int d\rho\, n_0(\rho) \left(m\rho - \frac{4}{3}\pi^2\rho^3 \bar{q}_R q_L \right), \tag{18}$$

where $n_0(\rho)$ is the tunneling rate. Note that the zero mode contribution acts like a mass term. For $N_f = 1$, there is only one chiral $U(1)$ symmetry, which is anomalous. This means that the anomaly breaks chiral symmetry and gives a fermion mass term. This is not true for more than one flavor. For $N_f = 2$, the result is

$$\mathcal{L}_{N_f=2} = \int d\rho\, n_0(\rho) \Big[\prod_f \left(m\rho - \frac{4}{3}\pi^2\rho^3 \bar{q}_{f,R} q_{f,L} \right) \tag{19}$$

$$+ \frac{3}{32} \left(\frac{4}{3}\pi^2\rho^3 \right)^2 \left(\bar{u}_R \lambda^a u_L \bar{d}_R \lambda^a d_L - \bar{u}_R \sigma_{\mu\nu} \lambda^a u_L \bar{d}_R \sigma_{\mu\nu} \lambda^a d_L \right) \Big].$$

One can easily check that the interaction is $SU(2) \times SU(2)$ invariant, but $U(1)_A$ is explicitly broken. This Lagrangian is of the type first studied by Nambu and Jona-Lasinio [13] and widely used as a model for chiral symmetry

breaking and as an effective description for low energy chiral dynamics. It can be transformed to the form discussed above when we compared it to NJL interaction.

2.5 *The quark condensate in the mean field approximation*

We showed in the last section that in the presence of light fermions, tunneling can only take place if the tunneling event is accompanied by N_f fermions which change their chirality. But in the QCD vacuum, chiral symmetry is broken and the quark condensate $\langle\bar{q}q\rangle = \langle\bar{q}_L q_R + \bar{q}_R q_L\rangle$ is non-zero. This means that there is a finite amplitude for a quark to change its chirality and we expect the instanton density to be finite.

For a sufficiently dilute system of instantons, we can estimate the instanton density in full QCD from the expectation value of the $2N_f$ fermion operator in the effective Lagrangian (19). Using the factorization assumption [5], we find that the factor $\prod_f m_f$ in the instanton density should be replaced by $\prod_f m_f^*$, where the effective quark mass is given by

$$m_f^* = m_f - \frac{2}{3}\pi^2\rho^2\langle\bar{q}_f q_f\rangle. \tag{20}$$

This shows that if chiral symmetry is broken, the instanton density is finite in the chiral limit.

This obviously raises the question whether the quark condensate itself can be generated by instantons. This question can be addressed using several different techniques (for a review, see [2, 3]). One possibility is to use the effective interaction (19) and to calculate the quark condensate in the mean field (Hartree-Fock) approximation. This correspond to summing the contribution of all "cactus" diagrams to the full quark propagator. The result is a gap equation [14]

$$\int \frac{d^4k}{(2\pi)^4}\frac{M^2(k)}{k^2+M^2(k)} = \frac{N}{4N_cV}, \tag{21}$$

which determines the constituent quark mass $M(0)$ in terms of the instanton density (N/V). Here, $M(k) = M(0)k^2\varphi'^2(k)/(2\pi\rho)$ is the momentum dependent effective quark mass and $\varphi'(k)$ is the Fourier transform of the zero mode profile [14]. The quark condensate is given by

$$\langle\bar{q}q\rangle = -4N_c\int\frac{d^4k}{(2\pi)^4}\frac{M(k)}{M^2(k)+k^2}. \tag{22}$$

Using our standard parameters $(N/V) = 1\,\mathrm{fm}^{-4}$ and $\rho = 1/3$ fm, one finds $\langle\bar{q}q\rangle \simeq -(255\,\mathrm{MeV})^3$ and $M(0) = 320$ MeV. Parametrically, $\langle\bar{q}q\rangle \sim (N/V)^{1/2}\rho^{-1}$ and $M(0) \sim (N/V)^{1/2}\rho$. Note that both quantities are not proportional to (N/V), but to $(N/V)^{1/2}$. This is a reflection of the fact that spontaneous breaking of chiral symmetry is not a single instanton effect, but involves infinitely many instantons.

A very instructive way to study the mechanism for chiral symmetry breaking at a more microscopic level is by considering the distribution of eigenvalues of the Dirac operator. A general relations that connects the spectral density $\rho(\lambda)$ of the Dirac operator to the quark condensate was given by Banks-Casher relation

$$\langle\bar{q}q\rangle = -\pi\rho(0). \tag{23}$$

This result is analogous to the Kondo formula for the electrical conductivity. Just like the conductivity is given by the density of states at the Fermi surface, the quark condensate is determined by the level density at zero virtuality λ. For a disordered, random, system of instantons the zero modes interact and form a band around $\lambda = 0$. As a result, the eigenstates are delocalized and chiral symmetry is broken. On the other hand, if instantons are strongly correlated, for example bound into topologically neutral molecules, the eigenvalues are pushed away from zero, the eigenstates are localized and chiral symmetry is unbroken. As we will see below, precisely which scenario is realized depends on the parameters of the theory, like the number of light flavors and the temperature. Of course, for "real" QCD with two light flavors at $T = 0$, we expect chiral symmetry to be broken. This is supported by numerical simulations of the partition function of the instanton liquid, see [2].

2.6 The Qualitative Picture of the Instanton Ensemble

Using basically such expressions and the known value of the quark condensate it was pointed out in[6] that all would be consistent only if the typical instanton size happened to be significantly smaller than their separation[4], $R = n^{-1/4} \approx 1fm$, namely $\rho_{\max} \sim 1/3\,\mathrm{fm}$.

In Fig.(1) one can see lattice data on instanton size distribution, obtain by cooling of the original gauge fields. Similar distribution can also be

[4]Derived in turn from the gluon condensate and the topological susceptibility.

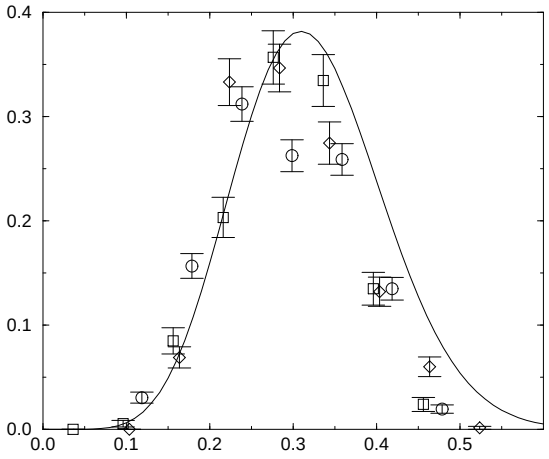

Figure 1: The instanton density $dn/d\rho d^4z$, [fm^{-5}] versus its size ρ [fm]. The points are from the lattice work [11], for this theory, with β=5.85 (diamonds), 6.0 (squares) and 6.1 (circles). Their comparison should demonstrate that results are rather lattice-independent. The line corresponds to one of the proposed expression $\sim exp(-2\pi\sigma\rho^2)$.

obtained from fermionic lowest Dirac eigenmodes: in this case no "cooling" is needed.

Let me now show another evidence for this value of the instanton size, taken from the pion form-factor calculated[16] in the instanton model. In Fig.(2) we show how the experimentally measured pion size correlates with the input mean instanton size: one can see from it that the value .35 fm is a clear winner.

With my current student, Pietro Faccioli, we are now working on the pion form-factor at larger momentum transfer, and have found that the agreement between the instanton-induced contribution and the monopole fit continues to at least $Q^2 \sim 10GeV^2$. At higher momentum transfers, the instanton term must die out, leaving the (probably undetectably small) perturbative asymptotics.

In summary, the following qualitative picture of the QCD vacuum have emerged:

1. Since the instanton size is significantly smaller than the typical separation R between instantons, $\rho/R \sim 1/3$, the vacuum is fairly dilute. The

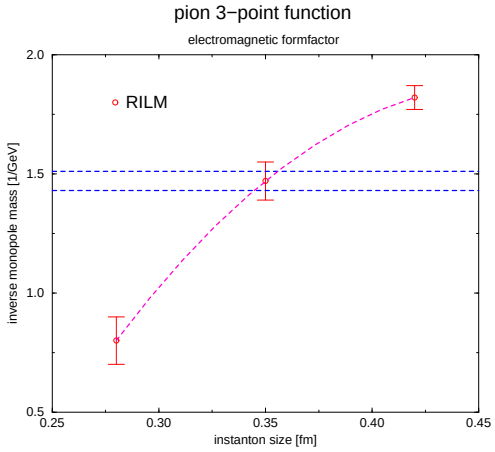

Figure 2: The fitted parameter M of the pion form-factor $ff \sim M^2/(Q^2+M^2)$ versus the inputed instanton size.

fraction of spacetime occupied by strong fields is only a few percent.

2. The fields inside the instanton are very strong, $G_{\mu\nu} \gg \Lambda^2_{QCD}$. This means that the semi-classical approximation is valid, and the typical action is large

$$S_0 = 8\pi^2/g^2(\rho) \sim 10 - 15 \gg 1. \tag{24}$$

Higher order corrections are proportional to $1/S_0$ and presumably small.

3. Instantons retain their individuality and are not destroyed by interactions. From the dipole formula, one can estimate

$$|\delta S_{int}| \sim (2-3) \ll S_0. \tag{25}$$

4. Nevertheless, interactions are important for the structure of the instanton ensemble, since

$$\exp|\delta S_{int}| \sim 20 \gg 1. \tag{26}$$

This implies that interactions have a significant effect on correlations among instantons, and the instanton ensemble in QCD is not a dilute gas but an *interacting liquid*.

The aspects of the QCD vacuum for which instantons are most important are those related to light fermions. Their importance in the context of chiral symmetry breaking is related to the fact that the Dirac operator has a chiral zero mode in the field of an instanton. These zero modes are localized quark states around instantons, like atomic states of electrons around nuclei. At finite density of instantons those states can become collective, like atomic states in metals. The resulting de-localized state corresponds to the wave function of the quark condensate.

Direct tests of all these ideas on the lattice are possible. One may have a look at the lowest eigenmodes and see if they are related to instantons or something else (monopoles, vortices...) by identifying their shapes - 4d bumps (lines or 2-d sheets) respectively. So far, only bumps (that is the instantons) were seen.

One may also test how locally chiral are the lowest eigenmodes. Just recently lattice practitioners learned how to get very accurate massless fermions on the lattice, and in a variety of ways: the domain wall method, the "perfect" actions or just empirically improved ones based on Wilson-Ginsparg relation. Let me refer to just few papers [25] which discuss those results, confirming the instanton model in its central prediction, that the majority of lowest eigenvectors of the QCD vacuum are made of instanton zero modes.

Let me now explain about the *lowest QCD scale* generated by instantons, mentioned above. The width of the *zero mode zone* of states is of the order of root-mean-square matrix element of the Dirac operator $< I|/D|J > \sim \rho^2/R^3$. Here states I,J are some instanton and anti-instanton zero modes, rho is the instanton size and $R \sim n^{-1/4} \approx 1fm$ is the distance between their centers. Note small factor $(\rho/R)^2 \sim 1/10$ here. The Dirac eigenvalues from the zone have similar magnitude. Now, the eigenvalues enter together with quark mass m: and so only when this quark mass is smaller than this scale we start seeing the physics of the zero mode zone. In particular, for *quenched* QCD (or instanton liquid) there is no determinant and the zone states have rather wrong spectrum. However, only if the quark mass is small compared to its width we start observing the difference. Only recently lattice practitioners were able to do so: indeed, quenched QCD results at small m start deviating from the correct answers quite drastically.

2.7 Interacting instantons

In the QCD partition function there are two types of fields, gluons and quarks, and so the first question one addresses is *which integral to take first.*

(i) One way is to eliminate *gluonic* degrees of freedom first. Physical motivation for this may be that gluonic states are heavy and an effective fermionic theory should be better suited to derive an effective low-energy fermionic theory. It is a well-trodden path and one can follow it to the development of a similar four-fermion theory, the NJL model. One can do simple mean field or random field approximation (RPA) diagrams, and find the mean condensate and properties of the Goldstone mesons[14]. The results for Color Super-conductors at high density reported below are done with the same technique as well. But nevertheless, not much can really be done in such NJL-like approach. In fact, multiple attacks during the last 40 years at the NJL model *beyond the mean field* basically failed. In particular, one might think that since baryons are states with three quarks, and one may wonder if using quasi-local four-fermion Lagrangians for the three body problem is a solvable quantum mechanical problem, and one can at least tell if nucleons are or are not bound in NJL. In fact it is not: the results depend strongly on subtleties of how the local limit for the interaction is defined, and there is no clear answer to this question. Other notorious attempts to sum more complicated diagrams deal with the possible modification of the the chiral condensate. Some works even claim that those diagrams destroy it *completely*!

Going from NJL to instantons improves the situation enormously: the shape of the form-factor is no longer a guess (it is provided by the shape of zero modes) and one can in principle evaluate any particular diagram. However *summing them all up* still seems like an impossible task.

(ii) The solution to this problem was found. For that one has to follow the opposite strategy and do the $fermion$ integral first. The first step is simple and standard: fermions only enter quadratically, leading to a fermionic determinant. In the instanton approximation, it leads to the Interacting Instanton Liquid Model, defined by the following partition function:

$$Z = \sum_{N_+,\,N_-} \frac{1}{N_+!N_-!} \int \prod_i^{N_+ + N_-} [d\Omega_i\, d(\rho_i)] \exp(-S_{\rm int}) \prod_f^{N_f} \det(\hat{D} + m_f)\,, \quad (27)$$

describing a system of pseudo-particles interacting via the bosonic action and the fermionic determinant. Here $d\Omega_i = dU_i\, d^4 z_i\, d\rho_i$ is the measure in

color orientation, position and size associated with single instantons, and $d(\rho)$ is the single instanton density $d(\rho) = dn_{I,\bar{I}}/d\rho dz$.

The gauge interaction between instantons is approximated by a sum of pure two-body interaction $S_{\rm int} = \frac{1}{2}\sum_{I\neq J} S_{\rm int}(\Omega_{IJ})$. Genuine three body effects in the instanton interaction are not important as long as the ensemble is reasonably dilute. Implementation of this part of the interaction (quenched simulation) is quite analogous to usual statistical ensembles made of atoms.

As already mentioned, quark exchanges between instantons are included in the fermionic determinant. Finding a diagonal set of fermionic eigenstates of the Dirac operator is similar to what people are doing, e.g., in quantum chemistry when electron states for molecules are calculated. The difficulty of our problem is however much higher, because this set of fermionic states should be determined for *all* configurations which appear during the Monte-Carlo process.

If the set of fermionic states is however limited to the subspace of instanton zero modes, the problem becomes tractable numerically. Typical calculations in the IILM involved up to N$\sim$ 100 instantons (+anti-instantons): which means that the determinants of $N \times N$ matrices are involved. Such determinants can be evaluated by an ordinary workstation (and even PC these days) so quickly that a straightforward Monte Carlo simulation of the IILM is possible in a matter of minutes. On the other hand, expanding the determinant in a sum of products of matrix elements, one can easily identify the sum of all closed loop diagrams up to order N in the 't Hooft interaction. Thus, in this way one can actually take care of about 100 factorial diagrams!

3 Lecture 2. Hadronic Structure and the QCD correlation functions.

3.1 Correlators as a bridge between hadronic and partonic worlds

Consider two currents separated by a $space-like$ distance x (which can be considered as the spatial distance, or an Euclidean time) and introduce correlation functions of the type

$$K(x) = < T(J(x)J(0)) > \tag{28}$$

with $J(x) = \bar{\psi}(x)\Gamma\psi(x)$. The matrix Γ contains γ_μ for vector currents, γ_5 for the pseudoscalar or 1 for the scalars, etc, and also a flavor matrix, if

needed.

We will start with isovector vector and axial currents, and then discuss 4 scalar-pseudoscalar channels: π (P=-1, I=1), σ or f_0 (P=+1,I=0), η (P=-1,I=0) and δ or a_0 (P=+1,I=1).

In a (relativistic) field theory, correlation functions of gauge invariant local operators are the proper tool to study the spectrum of the theory. The correlation functions can be calculated either from the physical states (mesons, baryons, glueballs) or in terms of the fundamental fields (quarks and gluons) of the theory. In the latter case, we have a variety of techniques at our disposal, ranging from perturbative QCD, the operator product expansion (OPE), to models of QCD and lattice simulations. For this reason, correlation functions provide a bridge between hadronic phenomenology on the one side and the underlying structure of the QCD vacuum on the other side.

Loosely speaking, hadronic correlation functions play the same role for understanding the forces between quarks as the NN scattering phase shifts did in the case of nuclear forces. In the case of quarks, however, confinement implies that we cannot define scattering amplitudes in the usual way. Instead, one has to focus on the behavior of gauge invariant correlation functions at short and intermediate distance scales. The available theoretical and phenomenological information about these functions was recently reviewed in [4].

In all cases at small x we expect $K(x) \approx K_0(x)$ where the latter corresponds to just *free* propagation of (about massless) light quarks. The zeroth order correlators are all just $K_0(x) = 12/(\pi^4 x^6)$, basically the square of the massless quark propagator.

The first deviations due to non-perturbative effects can be studied using Wilsonian Operator Product Expansion (OPE) in ref[5]. For all scalar and pseudoscalar channels the resulting first correction is

$$\frac{K(x)}{K_0(x)} = 1 + \frac{x^4}{384} < (gG)^2 > +... \tag{29}$$

The "gluon condensate" is assumed to be made out of a soft vacuum field, and therefore all arguments can be simply taken at the point $x = 0$. The so-called *standard* value of the "gluon condensate" appearing here was estimated previously from charmonium sum rules:

$$< (gG)^2 >_{SVZ} \approx .5\, GeV^4 \tag{30}$$

Thus, the OPE suggests the following scale, at which the correction becomes equal to the first term:

$$x_{OPE} = (384/ < (gG)^2 >_{SVZ})^{1/4} \approx 1.0\ fm \tag{31}$$

This seems to be completely consistent with the approximation used. However, as Novikov, Shifman, Vainshtein and Zakharov soon noticed[7], this (and other OPE corrections) completely failed to describe all the $J^P = O^{\pm}$ channels: we return to this issue after we consider vectors and axials.

3.2 Vector and axial correlators

The information available on vector correlation functions from experimental data on $e^+e^- -> hadrons$, the OPE and other exact results was reviewed in [4]. Since then, however, new high statistics measurement of hadronic τ decays $\tau \to \nu_\tau +$hadrons have been done. For definiteness, we use results of one of them, ALEPH experiment at CERN [17, 18].

The vector and axial-vector correlation functions are $\Pi_V(x) = \langle j_\mu^a(x) j_\mu^a(0)\rangle$ and $\Pi_A(x) = \langle j_\mu^{5\,a}(x) j_\mu^{5\,a}(0)\rangle$. Here, $j_\mu^a(x) = \bar{q}\gamma_\mu \frac{\tau^a}{2} q$, $j_\mu^{5\,a}(x) = \bar{q}\gamma_\mu\gamma_5 \frac{\tau^a}{2} q$ are the isotriplet vector and axial-vector currents. The Euclidean correlation functions have the spectral representation [4]

$$\Pi_{V,A}(x) = \int ds\, \rho_{V,A}(s) D(\sqrt{s}, x), \tag{32}$$

where $D(m,x) = m/(4\pi^2 x) K_1(mx)$ is the Euclidean coordinate space propagator of a scalar particle with mass m. We shall focus on the linear combinations $\Pi_V + \Pi_A$ and $\Pi_V - \Pi_A$. These combinations allows for a clearer separation of different non-perturbative effects. The corresponding spectral functions $\rho_V \pm \rho_A$ measured by the ALEPH collaboration are shown in Fig. 3. The errors are a combination of statistical and systematic ones (below we use them conservatively, as pure systematic): the main problem seems to be separation into V and A of channels with Kaons, which may affect $V - A$ at $s > 2\,GeV$ at 10% level. None of our conclusions are sensitive to it.

In QCD, the vector and axial-vector spectral functions must satisfy chiral sum rules. Assuming that $\rho_V - \rho_A = 0$ at above $s > m_\tau^2$, and using ALEPH data below it, one finds that all 4 of the sum rules are satisfied within the experimental uncertainty, but the central values differ significantly from the chiral predictions [17]. In general, both functions are expected to have oscillations of decreasing amplitude, and putting $\rho_V - \rho_A$ to zero at arbitrary

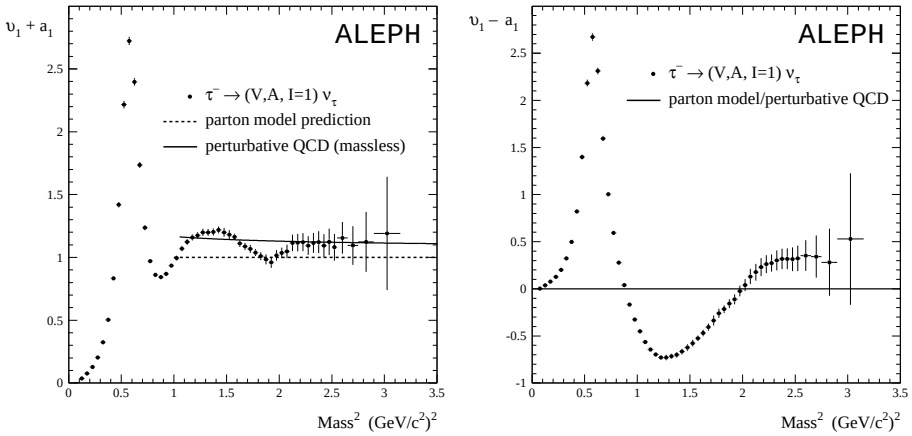

Figure 3: Spectral functions $v(s) \pm a(s) = 4\pi^2(\rho_V(s) + \rho_A(s))$ extracted by the ALEPH collaboration from *tau* lepton hadronic decays.

point imply appearance of spurious dimension $d = 2, 4$ operators in the correlation functions at small x. Therefore, we have decided to terminate the data above a specially tuned point, $s_0 = 2.5\,\mathrm{GeV}^2$, enforcing all 4 chiral sum rules. (The reader should however be aware of the fact that we have, in effect, slightly moved the data points in the small x region within the error band.) Finally we add the pion pole contribution (not shown in Fig. 3), which corresponds to an extra term $\Pi_A^\pi(x) = f_\pi^2 m_\pi^2 D(m_\pi, x)$. The resulting correlation functions $\Pi_V(x) \pm \Pi_A(x)$ are shown in Figs. 4.

We begin our analysis with the combination $\Pi_V - \Pi_A$. This combination is sensitive to chiral symmetry breaking, while perturbative diagrams, as well as gluonic operators cancel out.

In Fig. 4 we compare the measured correlation functions with predictions from the instanton liquid model (in its simplest form, random instanton liquid with parameters n, ρ fixed in [6] and discussed above).

The agreement of the instanton prediction with the measured $V - A$ correlation is impressive: it extends all the way from short to large distances. At distances $x > 1.25$ fm both combinations are dominated by the pion contribution while at intermediate x the ρ, ρ' and a_1 resonances contribute.

We shall now focus our attention on the $V + A$ correlation function. The unique feature of this function is the fact that the correlator remains close to free field behavior for distances as large as 1 fm. This phenomenon

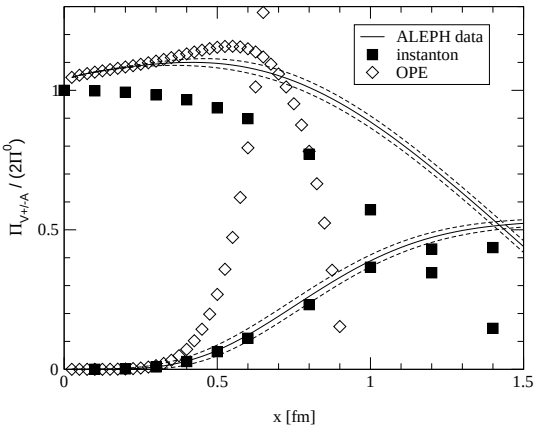

Figure 4: Euclidean coordinate space correlation functions $\Pi_V(x) \pm \Pi_A(x)$ normalized to free field behavior. The solid lines show the correlation functions reconstructed from the ALEPH spectral functions and the dotted lines are the corresponding error band. The squares show the result of a random instanton liquid model and the diamonds the OPE fit described in the text.

was referred to as "super-duality" in [4]. The instanton model reproduces this feature of the $V + A$ correlator. We also notice that for small x the deviation of the correlator in the instanton model from free field behavior is small compared to the perturbative $O(\alpha_2/\pi)$ correction. This opens the possibility of precision studies of the pQCD contribution. But before we do so, let us compare the correlation functions to the OPE prediction

$$\frac{\Pi_V(x) + \Pi_A(x)}{2\Pi_0(x)} = 1 + \frac{\alpha_s}{\pi} - \frac{1}{384}\langle g^2 G^2_{\mu\nu}\rangle x^4 - \frac{4\pi^3}{81}\alpha_s(x)\langle\bar{q}q\rangle \log(x^2) x^6 + \dots \qquad (33)$$

Note that the perturbative correction is attractive, while the power corrections of dimension $d = 4$ and $d = 6$ are repulsive. Direct instantons also induce an $O(x^4)$ correction $1 - \frac{\pi^2}{12}\left(\frac{N}{V}\right) x^4 + \dots$, which is consistent with the OPE because in a dilute instanton liquid we have $\langle g^2 G^2\rangle = 32\pi^2(N/V)$. This term can indeed be seen in the instanton calculation and causes the cor-

relator to drop below 1 at small x. It is possible to extract the value of Λ_{QCD} (we find $\alpha_s(m_\tau) = 0.35$) and even clear indication of running coupling. It is only possible to do because the non-perturbative corrections (represented by instantons) are basically cancelling each other to very high degree, in V+A channel.

Why is it happening? The first order in 't Hooft is indeed absent, due to chirality mismatch. There is no general theoretical reason why all non-perturbative of higher order should also do so: but ALEPH data used wrongly hint that they actually do so.

3.3 Spin-zero correlation functions

Now we will see cases which are completely opposite to those just considered: the instanton-induced effects would be large. Furthermore, the 4 channels actually show completely different non-perturbative deviation from K_0 at small x: half of them (π, σ) deviate upward, and another pair (η, δ) deviate downward.

But let me first demonstrate that the OPE scale determined above cannot be right. All we have to do is to evaluate the strength of the pion contribution to the correlator in question:

$$K_\pi(x) = \frac{\lambda_\pi^2}{4\pi^2 x^2} \tag{34}$$

The coupling constant is defined as $\lambda_\pi =< 0|J(0)|\pi >$ and the rest is nothing more than the scalar massless propagator[5]. Because both the pion term and the gluon condensate correction happen to be $1/x^2$, let us compare the coefficients. Ideal matching would mean they are about the same

$$\lambda_\pi^2 \approx \frac{< (gG)^2 >_{SVZ}}{8\pi^2} \tag{35}$$

The r.h.s. is about 0.0063 GeV^4. However, phenomenology tells us that (unlike the better known coupling to the axial current f_π) the coupling λ_π is surprisingly large[6]. The l.h.s. of this relation is actually $\lambda_\pi^2 = (.48\,GeV)^4 =$

[5]We can ignore the pion mass at the distances in question. We also ignore contributions of other states, which can only add positively to the correlator and made disagreement only worse.

[6]The reason for that is the the pion is rather compact and also the wave function is concentrated at its center, so that its value at $r = 0$ is large. We return to this point in the discussion of the "instanton liquid" model.

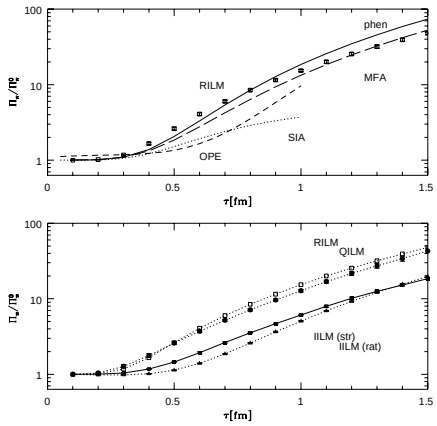

Figure 5: Pion correlation function in various approximations and instanton ensembles. In the top figure we show the phenomenological expectation (solid), the OPE (dashed), the single instanton (dash-dotted) and mean field approximations (dashed) as well as data in the random instanton ensemble. In the bottom figure we compare different instanton ensembles, random (open squares), quenched (circles) and interacting (streamline: solid squares, ratio ansatz solid triangles).

$0.053\,GeV^4$, about *10 times larger* than the r.h.s. It means much larger non-perturbative effect is needed to explain the deviation from the perturbative behavior.

Now, let us see why is it so. The instanton effects in spin-0 channels are in these cases much larger because effect of 't Hooft interaction appears in those cases in the first order. Furthermore, since it its flavor structure is non-diagonal $(\bar{u}u)(\bar{d}d)$ the correlator of two π^0 currents $(\bar{u}\gamma_5 u - \bar{d}\gamma_5 d)$ have it with opposite sign as compared to the correlator of η' currents $(\bar{u}\gamma_5 u + \bar{d}\gamma_5 d)$. What it means is that instantons are as attractive in the pion channel as they are repulsive in the η' case. The situation is reversed in the scalar channels: the isoscalar sigma is attractive and isovector is repulsive.

Full results from versions of the instanton liquid model for pion correlators are shown in fig.5. Different versions of the model (mentioned in figures below as IILM(rat) etc) differ by a particular ansatz for the gauge field used, from which the interaction is calculated. Note also, that these figures contain also a curve marked "phen": this is what the correlator actually looks like, according to phenomenology.

We simply show a few results of correlation functions in the different instanton ensembles (see original refs in[2]). Some of them (like vector and axial-vector ones) turned out to be easy: nearly any variant of the instanton

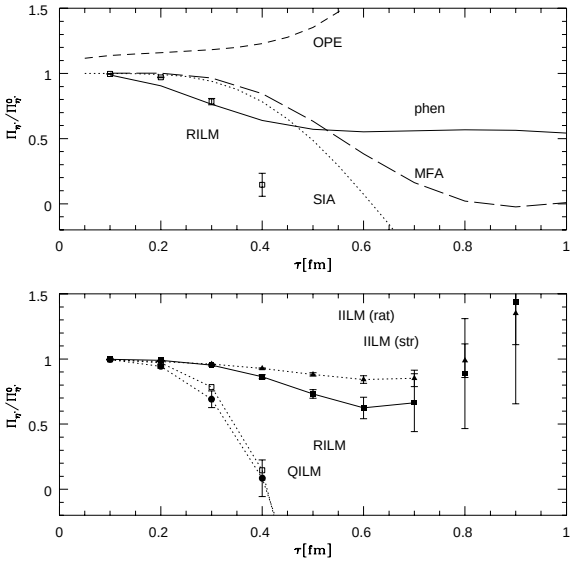

Figure 6: Eta prime meson correlation functions. The various curves and data sets are labeled as in Fig. 5. Note that random instanton liquid model (RILM) and quenched version (no fermionic determinant, only bosonic interactions) predict η' correlator to go negative. The same unphysical behavior has been found on the lattice.

model can reproduce the (experimentally known!) correlators well. Some of them are sensitive to details of the model very much: two such cases are shown in Figs. 5-6. The pion correlation functions in the different ensembles are qualitatively very similar. The differences are mostly due to different values of the quark condensate (and the physical quark mass) in the different ensembles. Using the Gell-Mann-Oaks-Renner relation, one can extrapolate the pion mass to the physical value of the quark masses. The results are consistent with the experimental value in the streamline ensemble (both quenched and unquenched), but clearly too small in the ratio ansatz ensemble. This is a reflection of the fact that the ratio ansatz ensemble is not sufficiently dilute.

The situation is drastically different in the η' channel. Among the ~ 40 correlation functions calculated in the random ensemble, only the η' and the isovector-scalar δ were found to be completely unacceptable. The correlation function decreases very rapidly and becomes *negative* at $x \sim 0.4$ fm. This behavior is incompatible even with a normal spectral representation. The interaction in the random ensemble is too repulsive, and the model "over-

explains" the $U(1)_A$ anomaly.

The results in the unquenched ensembles (closed and open points) significantly improve the situation. This is related to dynamical correlations between instantons and anti-instantons (topological charge screening). The single instanton contribution is repulsive, but the contribution from pairs is attractive. Only if correlations among instantons and anti-instantons are sufficiently strong are the correlators prevented from becoming negative. Quantitatively, the δ and $\eta_{\rm ns}$ masses in the streamline ensemble are still too heavy as compared to their experimental values. In the ratio ansatz, on the other hand, the correlation functions even show an enhancement at distances on the order of 1 fm, and the fitted masses are too light. This shows that the η' channel is very sensitive to the strength of correlations among instantons.

In summary, pion properties are mostly sensitive to global properties of the instanton ensemble, in particular its diluteness. Good phenomenology demands $\bar{\rho}^4 n \simeq 0.03$, as originally suggested in[6]. The properties of the ρ meson are essentially independent of the diluteness, but show sensitivity to $\bar{I}I$ correlations. These correlations become crucial in the η' channel.

3.4 Baryonic correlation functions

The existence of a strongly attractive interaction in the pseudoscalar quark-antiquark (pion) channel also implies an attractive interaction in the scalar quark-quark (diquark) channel. This interaction is phenomenologically very desirable, because it immediately explains why the nucleon is light, while the delta (S=3/2,I=3/2) is heavy.

The so called Ioffe currents (with no derivatives and the minimum number of quark fields) are local operators which can excite states with nucleon quantum numbers. Those with positive parity and spin 1/2 can also be represented in terms of scalar and pseudoscalar diquarks

$$\eta_{1,2} = (2,4)\left\{\epsilon_{abc}(u^a C d^b)\gamma_5 u^c \mp \epsilon_{abc}(u^a C\gamma_5 d^b)u^c\right\}. \qquad (36)$$

Nucleon correlation functions are defined by $\Pi^N_{\alpha\beta}(x) = \langle\eta_\alpha(0)\bar{\eta}_\beta(x)\rangle$, where α,β are the Dirac indices of the nucleon currents. In total, there are six different nucleon correlators: the diagonal $\eta_1\bar{\eta}_1$, $\eta_2\bar{\eta}_2$ and off-diagonal $\eta_1\bar{\eta}_2$ correlators, each contracted with either the identity or $\gamma\cdot x$. Let us focus on the first two of these correlation functions (for more detail, see[2] and references therein).

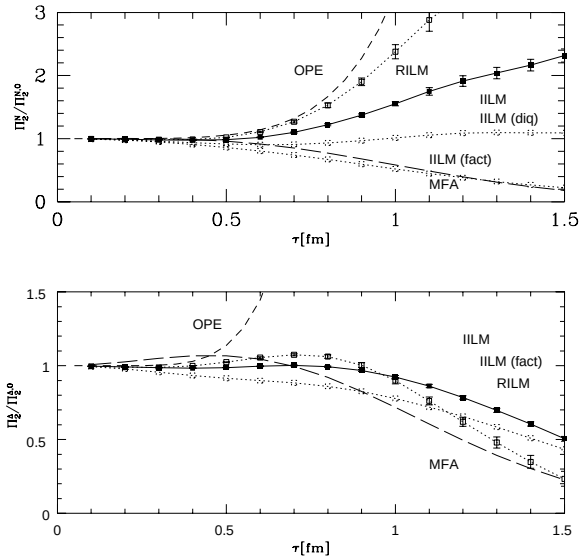

Figure 7: Nucleon and delta correlation functions Π_2^N and Π_2^Δ. Curves labeled as in Figs.on mesonic correlators.

The correlation function Π_2^N in the interacting ensemble is shown in Fig. 7. The fact that the nucleon in IILM is actually bound can also be demonstrated by comparing the full nucleon correlation function with that of three non-interacting quarks (the cube of the average propagator). The full correlator is significantly larger than the non-interacting one.

There is a significant enhancement over the perturbative contribution which is nicely described in terms of the nucleon contribution. Numerically, we find[7] $m_N = 1.019$ GeV. In the random ensemble, we have measured the nucleon mass at smaller quark masses and found $m_N = 0.96 \pm 0.03$ GeV. The nucleon mass is fairly insensitive to the instanton ensemble. However, the strength of the correlation function depends on the instanton ensemble. This is reflected by the value of the nucleon coupling constant, which is smaller in the IILM. In[19] we studied all six nucleon correlation functions. We showed that all correlation functions can be described with the same nucleon mass and coupling constants.

The fitted value of the threshold is $E_0 \simeq 1.8$ GeV, indicating that there is little strength in the "three quark continuum" (dual to higher resonances in

[7]Note that this value corresponds to a relatively large current quark mass $m = 30$ MeV.

the nucleon channel). A significant part of this interaction was traced down to the strongly attractive *scalar diquark* channel. The nucleon (at least in IILM) is a strongly bound diquark, plus a loosely bound third quark. The properties of this diquark picture of the nucleon continue to be disputed by phenomenologists. We will return to diquarks in the next section, where they will become Cooper pairs of Color Super-conductors.

In the case of the Δ resonance, there exists only one independent Ioffe current, given (for the Δ^{++}) by

$$\eta_\mu^\Delta = \epsilon_{abc}(u^a C\gamma_\mu u^b)u^c. \tag{37}$$

However, the spin structure of the correlator $\Pi^\Delta_{\mu\nu;\alpha\beta}(x) = \langle \eta^\Delta_{\mu\alpha}(0)\bar{\eta}^\Delta_{\nu\beta}(x)\rangle$ is much richer. In general, there are ten independent tensor structures, but the Rarita-Schwinger constraint $\gamma^\mu\eta^\Delta_\mu = 0$ reduces this number to four.

The mass of the delta resonance is too large in the random model, but closer to experiment in the unquenched ensemble. Note that,similar to the nucleon, part of this discrepancy is due to the value of the current mass. Nevertheless, the delta-nucleon mass splitting in the unquenched ensemble is $m_\Delta - m_N = 409$ MeV, larger but comparable to the experimental value 297 MeV. It mostly comes from the *absent scalar diquarks* in Δ channel.

4 Lecture 3. The Phases of QCD

4.1 The Phase Diagram

In this section we discuss QCD in extreme conditions, such as finite temperature/density. Let me first emphasize why it is interesting and instructive to do. It is not simply to practice once again the semi-classical or perturbative methods similar to what have been done before in vacuum. What we are looking for here are *new phases* of QCD (and related theories), namely new self-consistent solutions which differ qualitatively from what we have in the QCD vacuum.

One such phase occurs at high enough temperature $T > T_c$: it is known as Quark Gluon Plasma (QGP). It is a phase understandable in terms of basic quark and gluon-like excitations[38], without confinement and with unbroken chiral symmetry in the massless limit[8]. One of the main goals

[8]It does not mean though, that it is a simple issue to understand even the high-T limit of QCD, related to non-perturbative 3d dynamics.

of heavy ion program, especially at new the dedicated Brookhaven facility RHIC, is to study transitions to this phase.

Another one, which has been getting much attention recently, is the direction of finite density. Very robust Color Superconductivity was found to be the case here. Let me also mention one more frontier which has not yet attracted sufficient attention: namely a transition (or many transitions?) as the number of light flavors N_f grows. The minimal scenario includes a transition from the usual hadronic phase to a more unusual QCD phase, the *conformal* one, in which there are no particle-like excitations and correlators are power-like in the infrared. Even the position of the critical point is unknown. The main driving force of these studies is the intellectual challenge it provides.

The QCD phase diagram as we understand it now is shown in Fig 8(a), in the baryonic chemical potential μ (normalized per quark, not per baryon) and the temperature T plane. Some part of it is old: it has the hadronic phase at small values of both parameters, and QGP phase at large T,μ.

The phase transition line separating them most probably does not really start at $T = T_c, \mu = 0$ but at an "endpoint" E, a remnant of the so called QCD tricritical point which QCD has in the chiral (all quarks are massless) limit. Although we do not know where it is[9], we hope to find it one day in experiment. The proposed ideas rotate around the fact that the order parameter, the VEV of the sigma meson, is at this point truly massless, and creates a kind of "critical opalecence". Similar phenomena were predicted and then indeed observed at the endpoint of another line (called M from multi-fragmentation), separating liquid nuclear matter from the nuclear gas phase.

The large-density (and low-T) region looks rather different from what was shown at conferences just a year ago: two new Color Super-conducting phases appear there. Unfortunately heavy ion collisions do not cross this part of the phase diagrams and so it belongs to neutron star physics.

Above I mentioned an approach to high density starting from the vacuum. One can also work out in the opposite direction, starting from very large densities and going down. Since the electric part of one-gluon exchange is screened, and therefore the Cooper pairs appear due to magnetic forces. It is interesting by itself, as a rare example: one has to take care of *time delay effects* of the interaction. The result is indefinitely growing gaps at

[9]Its position is very sensitive to the precise value of the strange quark mass m_s

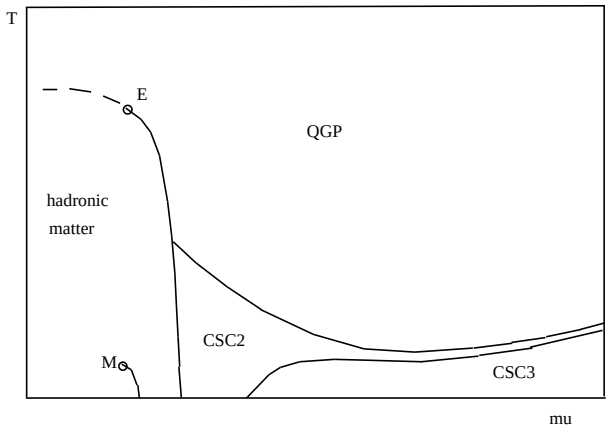

Figure 8: Schematic phase diagram of QCD, in temperature T- baryon chemical potential μ plane. E and M show critical endpoints of first order transitions: M (from multi-fragmentation) is that for liquid-gas transition in nuclear matter. The color superconducting phases, CSC2 and CSC3 are explained in the text.

large $\mu > 10GeV$, as [34] $\Delta \sim \mu exp(-\frac{3\pi^2}{\sqrt{2}g(\mu)})$.

4.2 Finite Temperature transition and Large Number of Flavors

There is no place here to discuss in detail the rather extensive lattice data available now, and I only mention some results related to instantons. In the vacuum a quasi-random set of instantons leads to chiral symmetry breaking and quasi-zero modes: but what in the same terms does the high-T phase look like?

The simplest solution would be just *suppression* of instantons at $T > T_c$, and at some early time people thought this is what actually happens. However, it should not be like this because the Debye screening which is killing them only appears at $T = T_c$. Lattice data works have also found no depletion of the instanton density up to $T = T_c$.

On the other hand, the absence of the condensate and quasi-zero modes implies that the "liquid" is now broken into finite pieces. The simplest of them are pairs, or the instanton-anti-instanton molecules. This is precisely what instanton simulations have found[2], see fig.9. Whether it is indeed so on the lattice is not yet clear: nice molecules were located, but the evidence for the molecular mechanism of chiral restoration is still far from being con-

vincing. (No alternative I am aware of have been so far proposed, though.)

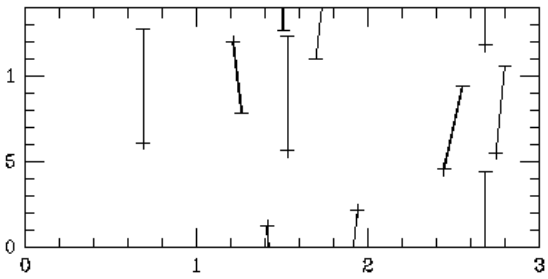

Figure 9: Typical configuration from instanton liquid simulation, at $T > T_c$. Lines indicate the direction in which quark propagators are the largest. Clear pairing of instantons and instantons are observed: the pairs tend to have the same spatial position and being separated mostly by Euclidean time.

The results of IILM simulations with variable number of flavors $N_f = 2, 3, 5$[10] flavors with equal masses can be summarized as follows. For $N_f = 2$ there is a second order phase transition which turns into a line of first order transitions in the $m - T$ plane for $N_f > 2$. If the system is in the chirally restored phase ($T > T_c$) at $m = 0$, we find a discontinuity in the chiral order parameter if the mass is increased beyond some critical value. Qualitatively, the reason for this behavior is clear. While increasing the temperature increases the role of correlations caused by fermion determinant, increasing the quark mass has the opposite effect. We also observe that increasing the number of flavors lowers the transition temperature. Again, increasing the number of flavors means that the determinant is raised to a higher power, so fermion induced correlations become stronger. For $N_f = 5$ we find that the transition temperature drops to zero and the instanton liquid has a chirally symmetric ground state, provided the dynamical quark mass is less than some critical value. Studying the instanton ensemble in more detail shows that in this case, all instantons are bound into molecules.

Unfortunately, little is known about QCD with large numbers of flavors from lattice simulations. There are data by the Columbia group for $N_f = 4$. The most important result is that chiral symmetry breaking effects were found to be drastically smaller as compared to $N_f = 0, 2$. In particular, the mass splittings between chiral partners such as $\pi - \sigma$, $\rho - a_1$, $N(\frac{1}{2}^+) - N(\frac{1}{2}^-)$,

[10]The case $N_f = 4$ is omitted because in this case it is very hard to determine whether the phase transition happens at $T > 0$.

extrapolated to $m = 0$ were found to be 4-5 times smaller. This agrees well with what was found in the interacting instanton model: more work in this direction is certainly needed.

4.3 High Density and Color Superconductivity

Although the idea of color superconductivity originates from 70's, the field of high density QCD was in the dormant state for long time till two papers [20, 21] (posted on the same day) in 1998 have claimed gaps about 100 times larger than previously thought. The field is booming since, as one can see from about 250 citations in 2 years those papers got.

Then-Princeton group (Alford-Rajagopal-Wilczek) have been thinking about different pairings from theory perspective, but our (Stony Brook) team (Rapp,Schafer,ES,Velkovsky) had started from the impressive qq pairing phenomenon found theoretically [19] in the instanton liquid model *inside the nucleon*. As explained above, we have found it to be, roughly speaking, a small drop of CS matter, made of one Cooper pair of sort (the *ud scalar diquark*) and one massive quark[11] . T.Schafer heroically attempted numerical simulations of the instanton liquid model at finite μ: although he was not very successful[12] he found out strange "polymers" made of instantons connecting by 2 through going quark lines. It take us some time to realize we see paths of condensed diquarks! It was like finding superconductivity by watching electrons moving on your computer screen.

The main point I would like to emphasize here is that the qq pairing of such diquarks have in fact deep dynamical roots: it follows from the same basic dynamics as the "superconductivity" of the QCD vacuum, the chiral (χ-)symmetry breaking. These spin-isospin-zero diquarks are related to pions, as we will see below.

The most straightforward argument for deeply bound diquarks came from the bi-color ($N_c = 2$) theory: in it the scalar diquark is degenerate with pions. By continuity from $N_c = 2$ to 3, a trace of it should exist in real QCD[13].

Instantons create the following amusing *triality*: there are three attractive channels which compete: (i) the instanton-induced attraction in $\bar{q}q$ chan-

[11] As opposed to Δ (decuplet) baryons, which is a small drop of "normal" quark matter, without scalar diquarks.

[12] for the same reason as lattice people cannot do it: the fermionic determinant is not real.

[13] Instanton-induced interaction strength in diquark channel is $1/(N_c - 1)$ of that for $\bar{q}\gamma_5 q$ one. It is the same at $N_c = 2$, zero for large N_c, and is exactly in between for $N_c = 3$.

nel leading to χ-symmetry breaking. (ii) The instanton-induced attraction in qq which leads to color superconductivity. (iii) The *light-quark-induced* attraction of $\bar{I}I$, which leads to pairing of instantons into "molecules" and a Quark-Gluon Plasma (QGP) phase without *any* condensates.

At very high density we also can find *arbitrarily dilute instanton liquid*, as shown recently in [35]. The reason it cannot exist in vacuum or high T is that if instanton density goes below some critical value, the cannot be any condensate. (The system then breaks into instanton molecules or other clusters and chiral symmetry is restored.) However at high density the superconducting condensate can be created perturbatively as well (we mentioned it above) and there is no problem. The dilute instantons interact by exchanging very light η' (which would be massless without instantons): one can calculate effective Lagrangian, theta angle dependence etc.

Bi-color QCD: a very special theory One reason it is special (well known to to the lattice community): its fermionic determinant is *real* even for non-zero μ, which makes simulations possible. However the major interest in this theory is related the so called *Pauli-Gursey symmetry.* We have argued above that pions and diquarks appear at the same one-instanton level, and are so to say brothers. In bi-color QCD they becomes identical twins: due to the additional symmetry mentioned the diquarks are *degenerate* with mesons.

In particular, chiral symmetry breaking is done like this $SU(2N_f) \to Sp(2N_f)$, and for $N_f = 2$ the coset $K = SU(4)/Sp(4) = SO(6)/SO(5) = S^5$. Those 5 massless modes are pions plus the scalar diquark S and its anti-particle $\bar{S}$.

Vector diquarks are degenerate with vector mesons, etc. Therefore, the scalar-vector splitting is in this case about twice the constituent quark mass, or about 800 MeV. It should be compared to binding in the "real" $N_c = 3$ QCD of only 200-300 MeV, and to zero binding in the large-N_c limit.

The corresponding sigma model describing this χ-symmetry breaking was worked out in[20]: for further development see[22]. As argued in [20], in this theory the critical value of the transition to Color Superconductivity is simply $\mu = m_\pi/2$, or zero in the chiral limit. The diquark condensate is just a rotated $< \bar{q}q >$ one, and the gap is the constituent quark mass. Recent lattice works [26] display it in great detail, building confidence for other cases.

New studies reveal possible new crystalline phases. These phases still have somewhat debatable status, so I have not indicated them on the

phase diagram.

Once again, there were two papers submitted by chance on the same day. The "Stony Brook" team[23] have found that a "chiral crystal" with oscillating $< \bar{q}q(x) >$ (similar to Overhouser spin waves in solid state) can compete with the BCS 2-flavor superconductor at its onset, or $\mu \approx 400\, MeV$. The proper position of this phase is somewhere in between the hadronic phase (with constant $< \bar{q}q >$) and color superconductor.

The "MIT group"[24] have looked at the oscillating superconducting condensate $< qq(x) >$, following earlier works on the so called LOFF phase in usual superconductors. They have found that it is appearing when the difference between Fermi momenta of different quark flavors become comparable to the gap. The natural place for it on the phase diagram is close to the line at which color superconductivity disappears because the gap goes to zero.

5 Lecture 4.High Energy Collisions of Heavy Ions

5.1 The Little Bang: AGS, SPS and now the RHIC era

Let me start with brief comparison of these two magnificent explosions: the Big Bang versus the Little Bang, as we call heavy ion collisions.

The expansion law is roughly the Hubble law in both, $v(r) \sim r$ although strongly anisotropic in the Little Bang. The Hubble constant tells us the expansion rate today: similarly radial flow tells us the final magnitude of the transverse velocity. The acceleration history is not really well measured. For Big Bang people use distance supernovae, we use Ω^- which does not participate at the late stages to learn *what was the velocity earlier*. Both show small dipole (quadrupole or elliptic for Little Bang) components which has some physics, and who knows maybe we will see higher harmonics fluctuations later on, like in Universe. As we will discuss below, in both cases the major puzzle is how this large entropy has been actually produced, and why it happened so early.

The major lessons we learned from AGS experiments ($E_{LAB} = 2 - 12 AGeV$) are:
(i) Strangeness enhancement over simple multiple NN collisions appear from very low energies, and heavy ion collisions quickly approach nearly ideal chemical equilibrium of strangeness.
(ii) "Flows" of different species, in their radial,directed and elliptical form, are in this energy domain driven by collective potentials and absorptions:

they are not really flows in hydro sense. All of them strongly diminish by the high end of the AGS region, demonstrating the onset of "softness" of the EoS. Probably it is some precursor of the QCD phase transition.

Several important lessons came so far from CERN SPS data:
(i) Much more particle ratios have been measured there: overall those show surprisingly good degree of chemical equilibration: the chemical freeze-out parameters are tantalizingly close to the QGP phase boundary.
(ii) Dileptons show that radiation spectral density is very different in dense matter compared to ideal hadronic gas. The most intriguing data are CERES finding of "melting of the ρ", which seem to be transformed into a wide continuum reaching down to invariant masses as low as 400 MeV. It puts in doubt "resonance gas" view of hadronic matter at these conditions. Intermediate mass dileptons studied by NA50 can be well described by thermal radiation with QGP rates.
(iii) The impact parameter of J/ψ and ψ' suppression in PbPb collisions studied by NA50 collaboration shows rather non-trivial behavior. More studies are needed, including especially measurements of the open charm yields, to understand the origin and magnitude of the suppression.

However, during last several months those discussions have been overshadowed by a list of news from RHIC, Relativistic Heavy Ion Collider at Brookhaven National Laboratory. It had its first run in summer 2000 and reported recently at Quark Matter 2001 conference [27]: many details are discussed in Prof.M.Gylassy's lectures.

A brief summary is as follows. These results have shown that heavy ions collisions (AA) at these energies significantly differ *both* from the pp collisions at high energies and the AA collisions at lower (SPS/AGS) energies. The main features of these data are quite consistent with the Quark-Gluon Plasma (QGP) (or Little Bang) scenario, in which entropy is produced promptly and subsequent expansion is close to adiabatic expansion of equilibrated hot medium.

(Let me mention here two other pictures of the heavy ion production, discuss prior to appearance of these data. One is the *string picture*, used in event generators like RQMD and UrQMD: they predicted effectively very soft EoS and elliptic flow decreasing with energy. The other one is *pure minijet scenario*, in which most secondaries would come from independently fragmenting minijets. If so, there are basically no collective phenomena whatsoever.)

Already the very first multiplicity measurements reported by PHOBOS

collaboration [47] have shown that particle production per participant nucleon is no longer constant, as was the case at lower (SPS/AGS) energies. This new component may be due to long-anticipated $pQCD$ processes, leading to perturbative production of new partons. Unlike high p_t processes resulting in visible jets, those must be undetectable *"mini-jets"* with momenta $\sim 1-2\,GeV$. Production and decay of such *mini-jets* was discussed in Refs [48], also this scenario is the basis of widely used event generator HIJING [46]. Its crucial parameter is the *cutoff scale* p_{min}: if fitted from pp data to be 1.5-2 GeV, it leads to predicted mini-jet multiplicity $dN_g/dy \sim 200$ for central AuAu collisions at $\sqrt(s) = 130\,AGeV$. If those fragment independently into hadrons, and are supplemented by "soft" string-decay component, the predicted total multiplicity was found to be in good agreement with the first RHIC multiplicity data. Because partons interact perturbatively, with their scattering and radiation being strongly peaked at small angles, their equilibration is expected to be relatively long [49]. However, new set of RHIC data reported in [27] have provided serious arguments *against* the mini-jet scenario, and point toward quite rapid entropy production rate and early QGP formation.

(i) If most of mini-jets fragment independently, there is no *collective phenomena* such as transverse flow related with the QGP pressure. However, it was found that those effects are very strong at RHIC. Furthermore, STAR collaboration have observed very robust *elliptic flow* [37], which is in perfect agreement with predictions of hydrodynamical model [43, 42] assuming equilibrated QGP with its full pressure $p \approx \epsilon/3$ above the QCD phase transition. This agreement persists to rather peripheral collisions, in which the overlap almond-shaped region of two nuclei is only a couple fm thick. STAR and PHENIX data on spectra of identified particles, especially $p, \bar{p}$, indicate spectacular radial expansion, also in agreement with hydro calculations [43, 42]. (ii) Spectra of hadrons at large p_t, especially the π^0 spectra agree well with HIJING for peripheral collisions, but show much smaller yields for central ones, with rather different, (exponential-shaped) spectra. It means long-anticipated *"jet quenching"* at large p_t is seen for the first time, with a surprisingly large suppression factor $\sim 1/5$. Keeping in mind that jets originating from the surface outward cannot be quenched, the effect seem to be as large as it can possibly be. For that to happen, the outgoing high-p_t jets should propagate through matter with parton population larger than the abovementioned minijet density predicted by HIJING.

(iii) Curious interplay between collective and jet effects have also been

studied by STAR collaboration, in form of elliptic asymmetry parameter $v_2(p_t)$. At large transverse momenta $p_t > 2\,GeV$ the data depart from hydro predictions and levels off. When compared to predictions of jet quenching models worked out in [50], they also indicate gluon multiplicity several times larger than HIJING prediction, and are even consistent with its maximal possible value evaluated from the final entropy at freeze-out, $(dN/dy)_\pi \sim 1000$.

5.2 Collective flows and EoS

If we indeed have produced excited matter (rather than just a bunch of partons which fly away and fragment independently), we expect to see certain collective phenomena. Ideally, those should be quantitatively reproduced by relativistic hydrodynamics which is basically just local energy-momentum conservation plus the EoS we know from the lattice and models.

The role of the QCD phase transition in matter expansion is significant. QCD lattice simulations [40] show approximately 1st order transition. Over a wide range of energy densities $e = .5 - 1.4\,GeV/fm^3$ the temperature T and pressure p are nearly constant. So the ratio of pressure to energy density, p/e, decreases till a minimum at particular energy density $e_{sp} \approx 1.4\,GeV/fm^3$, known as the *softest point* [41]. Near e_{sp} small pressure gradient can not effectively accelerate the matter and the evolution stagnates. However when the initial energy density is well above the QCD phase transition region, $p/e \approx 1/3$, and this pressure drives the collective motion. The energy densities reached at time $\sim 1fm/c$ at SPS($\sqrt{s}_{NN} = 17\,GeV$) and RHIC ($\sqrt{s}_{NN} = 130\,GeV$) are about 4 and 8 GeV/fm^3, respectively. We found that at RHIC conditions we are in the latter regime, and matter accelerates to $v \sim .2c$ *before* entering the soft domain. Therefore by freeze-out this motion changes the spatial distribution of matter dramatically: e.g. as shown in [36] the initial almond-shape distribution 10 fm/c later looks like two separated shells, with a little "nut" in between.

The simplest way to see hydro expansion is in spectra of particles: on top of chaotic thermal distributions $\sim exp(-m_t/T), m_t^2 = p_t^2 + m^2$ one expect to see additional broadening due to hydro outward motion. This effect is especially large if particles are heavy, since flow with velocity v add momentum mv.

Derek Teaney [43] have developed a comprehensive Hydro-to-Hadrons (H2H) model combines the hydrodynamical description of the initial QGP/

mixed phase ($e > .5GeV/fm^3$) stages, where hadrons are not appropriate degrees of freedom, with a hadronic cascade RQMD for the hadronic stage. In this way, we can include different EoS displaying properties of the phase transition, and also incorporate complicated final state interaction at freeze-out. The set of EoS used is shown in Fig.10.

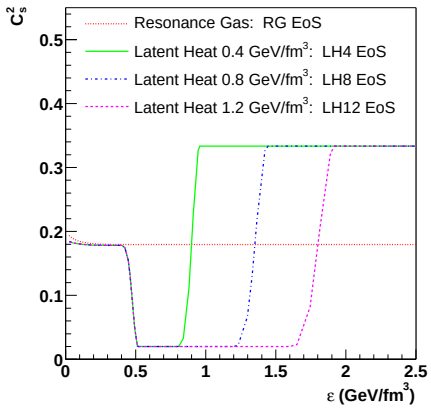

Figure 10: The EoSs in form squared speed of sound $c^2 = dp/d\epsilon$ with variable Latent Heats $.4GeV/fm^3$, $.8GeV/fm^3$,.. labeled as LH4, LH8,..versus the energy density.

Radial flow is usually characterized by the slope parameter T: each particle spectra are fitted to the form $dN/dp_t^2dy \sim exp(-m_t/T), m_t^2 = p_t^2 + m^2$.Although we denoted the slope by T, it is *not* the temperature: it incorporates random thermal motion and collective transverse velocity. The SPS NA49 slope parameters for pion and protons are shown in Fig. 11(a). Parameter T grows with particle multiplicity due to increased velocity of the radial flow. Furthermore, the rate of growth depends on the EoS: the softer it is, the less growth. The SPS NA49 data correspond to two data points (our fits to spectra) favor the (relatively stiff) LH8 EoS. (Details of the fit, discussion of the b-dependence etc see in [43].) It is very important to get these parameters for RHIC, especially for heavy secondaries like nucleons and hyperons.

For $non-central$ collisions the overlap region in the transverse plane has an elliptic, "almond", shape, and larger pressure gradient force matter to expands preferentially in the direction of the impact parameter [39]. Compared to radial flow, the elliptic flow is formed earlier, and therefore it measures the early pressure. The *elliptic flow* is quantified experimentally by measuring

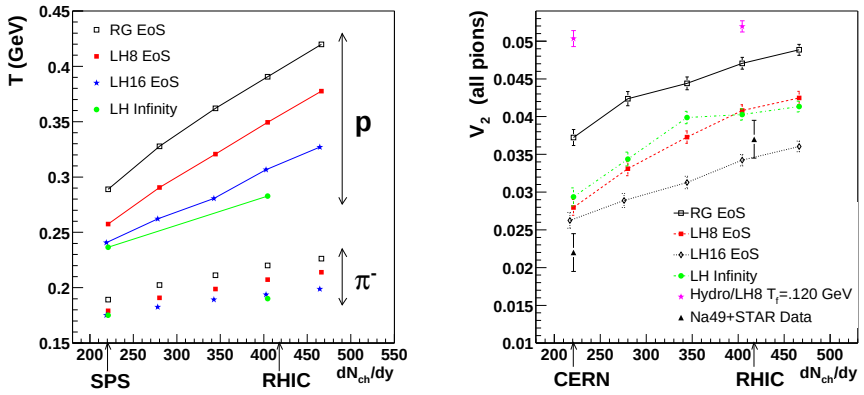

Figure 11: The transverse mass slope T (a) and elliptic flow parameter V_2 (b) versus midrapidity (y=0) charged purticle multiplicity, for AuAu collisions with b=6.

the azimuthal distributions of the produced particles and calculating the elliptic flow parameter $V_2 = \langle cos(2\phi) \rangle$ where ϕ angle is measured with respect to the impact parameter direction, around the beam axis. It appears due to the elliptic *spatial* deformation of the overlap region in the nucleus-nucleus collision, quantified by its eccentricity $\epsilon_2 =< y^2 - x^2 > / < x^2 + y^2 >$, usually calculated in Glauber model. Since the effect (v_2) is proportional to the cause (ϵ_2), the ratio v_2/ϵ_2 does not have strong dependence on the impact parameters b, and this ratio is often used for comparison. (We would not do that below, in the detailed comparison to data, because $\epsilon_2(b)$ is not directly measured.

In figure 11(b) the elliptic flow of the system is plotted as a function of charged particle multiplicity at an impact parameter of 6 fm. Before discussing the energy dependence, let us quantify the magnitude of elliptic flow at the SPS. Ideal relativistic hydrodynamics used in earlier works [39, 42] generally over-predicts elliptic flow by about factor 2. Example of such kind is indicated by a star in figure 11(b): it is our hydro result (with LH8 EoS) which has been followed hydrodinamically till very late stages, the freeze-out temperature $T_f = 120\, MeV$. By switching to hadronic cascade at late stages, we have more appropriate treatment of resonance decays and re-scattering rate, and so one can see that it significantly reduces V_2, to the range much closer to the data points.

One might thing that one can also do that by simply taking *softer* EoS,

e.g. increasing the latent heat. However, it only happens till LH16 and then v_2 start even slightly increase again. The explanation of this non-monotonous behavior is the interplay of the initial "QGP push" for stiffer EoS, with longer time for hadronic stage available for softer EoS. We cannot show here details, but it turns out that a given (experimental) V_2 value can correspond to *two different solutions*, one with earlier push and another with the later expansion dominating. Coincidentally, STAR data point happen to be right at the onset of such a bifurcation, close to LH16. The *multiplicity dependence* of V_2 appears simple from figure 11(b): all curve show growth with about the same rate. Note however that such growth of V_2 from SPS to RHIC (first predicted in [44] where our first preliminary results has been shown) Is not shared by most other models. In particular, *string-based* models like UrQMD predicts a decrease by a factor of ≈ 2 [45]. It happens because strings produce no transverse pressure and so the effective EoS is super-soft at high energies. Models based on *independent parton scattering and decay* (such as HIJING) also predict basically vanishing (or slightly negative)[46] V_2.

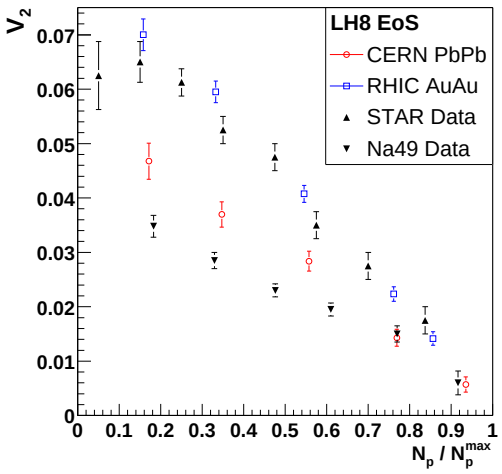

Figure 12: v2 versus impact parameter b, described experimentally by the number of participant nucleons, for RHIC STAR and SPS NA49 experiments. Both are compared to our results, for EoS LH8.

In Fig.12 we show how our results compare with data as a function of impact parameter. One can see that the agreement becomes much better at RHIC. Furthermore, one may notice that deviation from linear dependence we predict becomes visible at SPS for more peripheral collisions with $N_p/N_p^{max} < 0.6$ or so, while at RHIC only the most peripheral point, with $N_p/N_p^{max} = 0.05$ show such deviation. This clearly shows that hydrodynamical regime in general works much better at RHIC.

In summary, the flow phenomena observed at RHIC are stronger than at SPS. It is in complete agreement with the QGP scenario. All data on elliptic and radial flow can be nicely reproduced by the H2H model. Furthermore, we are able to restrict the EoS, to those with the latent heat about .8 GeV/fm^3.

5.3 How QGP happened to be produced/equilibrated so early?

One possible solution to the puzzle outlined above can be a *significantly lower cutoff scale* in AA collisions, as compared to $p_{min} = 1.5 - 2\,GeV$ fitted from the pp data. That increases perturbative cross sections, both due to smaller momenta transfer and larger coupling constant. As I argued over the years, the QGP is a new phase of QCD which is *qualitatively different* from the QCD vacuum: therefore the cut-offs of pQCD may have entirely different values and be determined by different phenomena. Furthermore, since QGP is a plasma-like phase which screens itself perturbatively [38], one may think of a cut-offs to be determined *self-consistently* from resummation of perturbative effects. These ideas known as *self-screening* or *initial state saturation* were discussed in Refs. [49]. Although the scale in question grows with temperature or density, *just above* T_c it may actually be *smaller* than the value 1.5-2 GeV we observe in the vacuum. Its first experimental manifestation may be dropping of the so called "duality scale" in the observed dilepton spectrum, see discussion in [52].

Another alternative to explain large gluon population at RHIC would be an existence of more rapid multi-gluon production processes. Let us consider an alternative *non−perturbative* scenario based entirely on non-perturbative processes involving *instantons* and *sphalerons* [51]. But before we do that, we have to take a look at hadronic collisions and briefly review few recent papers on the subject.

6 Lecture 5. Instanton-induced effects in high energy collisions

6.1 Why all hadronic cross sections grow with energy?

At $s > 10^3 GeV^2$ hadronic cross sections as $\bar{p}p, pp, \pi p, Kp$, γN and even $\gamma\gamma$ slowly grow with the collision energy s, approximately as $\sigma \sim s^{\Delta}$. This behavior can be parameterized by Regge phenomenology, with the leading role plaied by the so called *soft Pomeron*. We cannot describe here its long history, starting from Pomeranchuck and Gribov in 1960's. Phenomenologically it is still in very good shape. where a supercritical pole with the intercept $\Delta \sim 0.08$. Below TeV energies such growth can be well described by a simple logarithmically growing term

$$\sigma_{hh'}(s) = \sigma_{hh'}(s_0) + log(s/s_0) X_{hh'} \Delta + ... \tag{38}$$

and we will concentrate on its origin, ignoring both the higher powers of log(s) and other, decreasing, Regge terms. We will use those two parameters from PDG-2000 recent fits, the intercept and its coefficient in $pp, \bar{p}p$ collisions, $\Delta = \alpha(0) - 1 = 0.093(2)$, $X_{NN} = 18.951(27)\ mb$.

The physical origin of constant and logarithmically growing parts of the are different. The former can be explained by prompt color *exchanges*, as suggested by Low and Nussinov long ago. It nicely correlates with flux tube picture of the final state.

The *growing* part of the cross section cannot be generated by t-channel color exchanges and is associated with processes promptly producing some objects, with log(s) coming from the longitudinal phase space. In pQCD it is *gluon* production, by processes like the one shown in Fig.13(a). If iterated in the t-channel in ladder-type fashion, the result is approximately a BFKL pole [53]. Although the power predicted is much larger than Δ mentioned, it seem to be consistent with much stronger growth seen in hard processes at HERA: thus it is therefore sometimes called the "hard pomeron".

At this point I has been frequently asked: why is it so difficult to understand the growth of hadronic cross section, if HERA data shows spectacular increase of the gluonic number at small x? Shouldn't all these gluons collide with each other and naturally generate such growth?

The issue is not that simple, and the first thing to do at this point is to remind the reader about the scales involved. At large Q^2 we resolve the partons and see these magnificent rise toward the small x indeed: but high

energy hadron collisions do not proceed at such scale. In fact the scale is "semi-hard" $Q^2 \sim 1\,GeV$, as the Pomeron slope indicate. If we now go back to analysis of HERA/SLAC data and try to extract gluon density at this scale, we will not find a significant growth. What it indicates, is that all these multiple gluons actually add up into some coherent fields at such scale, which we do not yet understand.

The second issue has to do with the mutual screening of all these gluons. If the effective size of the hadron would not grow with energy, any number of interaction can only produce constant cross section of a black disk, without growth.

The physical origin of cross section growth remains an outstanding open problem: neither the perturbative resummations nor many non-perturbative models are really quantitative. It is hardly surprising, since scale at which soft Pomeron operates (as seen e.g. from the Pomeron slope $\alpha'(0) \approx 1/(2\,GeV)^2$) is also the "substructure scale" mentioned above.

There are basically three distinct approaches:

(i) *Minijet-based models* use familiar formulae from pQCD [48]. They are well-tested in the domain of hard jets, but their application at the semi-hard scale is a drastic extrapolation. All of these models assume the existence of a non-perturbative momentum cutoff, p_{cutoff}, in order to render pQCD results finite. This cutoff is left unexplained, treated as a purely phenomenological parameter, and all results depend greatly on its value.

(ii) *Instanton-based* dynamics, to be discussed below, have only recently been applied to high-energy scattering [28, 32, 29] and use insights obtained a decade ago in electroweak theory [33]. Particularly relevant for this work are the first two references, in which the growing part of the hadron-hadron cross sections is ascribed to multi-gluon production via instantons.

(iii) The *Color Glass Condensate*, a classical Weitzecker-Williams field of gluons carried by interacting hadrons, can be excited to produce prompt gluons [58]. This is another example of a weakly-coupled system involving non-perturbative gauge field configurations.

For long time people have constructed multi-peripheral models with ladders made of hadrons. Recent story started with Kharzeev and Levin[30] who kept t-channel gluons but tried to substitute the gluonic "rungs" of the BFKL ladder by those with a pair of pions, or sigma meson, to increase the cross section. They used the gg-$\pi\pi$ non-perturbative vertices known from the low energy theorem. Their estimated value for Δ was close to Δ_{phen}. Introducing *instantons* into the problem, I re-analyzed [31] the contribution

of the colorless scalar channel generated by operator $G^2_{\mu\nu}$, using the gg-$\pi\pi$ and gg$-scalar-glueball$ couplings determined previously from the calculation of appropriate Euclidean correlators, see [2]. The result turns out to reduce those of the KL paper, with $\Delta \approx 0.05$ only, and pions and glueball contributions being roughly equal.

6.2 "Soft" Pomeron from instantons

We put "soft" in quotation marks here because we do not entirely agree with this terminology. It is now clear that the Pomeron itself is a small object, with its size represented by the slope of its trajectory, $\alpha'(t=0) \approx 1/(4\,\mathrm{GeV}^2)$. The scale involved, 0.1 fm, is much smaller than hadronic radii, and so the Pomeron exchanges should in fact be treated on the level of individual partons, appropriately defined at the intermediate momentum scale of 1-2 GeV. For lack of a better standard term, we will refer to it as the *semi-hard* scale.

More precisely, we will not consider the nature of the soft Pomeron in full either. The leading Regge pole, if it exists, is the analog of a single bound state appearing (in t-channel),as a result of a rather different interactions[14]. Although existence of such pole is an attractive possibility, no general principles demand it to be true in real QCD.

Recent application of the instanton-induced dynamics to this problem have been discussed in several papers [54]. Especially relevant for this Letter are two last works which use insights obtained a decade ago in discussion of instanton-induced processes in electroweak theory [33], and the growing part of the hh cross sections were ascribed to multi-gluon production via instantons, see Fig.13(b). Among qualitative features of this theory is the explanation of why no odderon appears (instantons are SU(2) objects, in which quarks and antiquarks are not really distinct), an explanation of the small power Δ (it is proportional to "instanton diluteness parameter" $n\rho^4$ mentioned above), the small size of the soft Pomeron (governed simply by small size of instantons $\rho \sim 1/3\,fm$). Although instanton-induced amplitudes contain small "diluteness" factor, there is no extra penalty for production of new gluons: thus one should expect instanton effects to exceed perturbative amplitudes of sufficiently high order. This generic idea is also behind the present work, dealing with prompt multi-gluon production.

[14]For example, J/ψ is definite charmonium state, which appears as a result of an interplay of both perturbative and confining potentials.

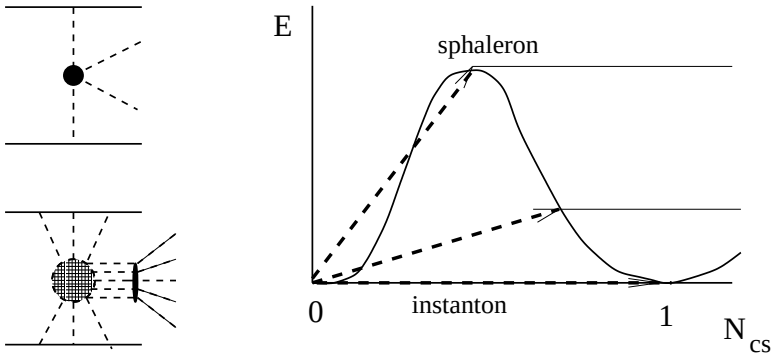

Figure 13: (a) A typical inelastic perturbative process (two t-channel gluons collide, producing a pair of gluons) to (b) non-perturbative inelastic process, incorporating collisions of few t-channel gluons with the instanton (the shaded circle), resulting in multi-gluon production. The bottom of the figure (c) shows the same process, but in a quantum mechanical way. The energy of Yang-Mills field versus the Chern-Simons number N_{cs} is a periodic function, with zeros at integer points. The *instanton* (shown by the lowest dashed line) is a transition between such points. However if some nonzero energy is deposited into the process during transition, the virtual path (the dashed line) leads to a *turning points*, from which starts the real time motion outside the barrier (shown by horizontal solid lines). The maximal cross section corresponds to the transition to the top of the barrier, called the *sphaleron*.

Technical description of the process can be split into two stages. The first (at which one evaluates the probability) is the motion *under the barrier*, and it is described by Euclidean paths approximated by instantons. Their interaction with the high energy colliding partons results in some energy deposition and subsequent motion *over the barrier*. Furthermore, the intermediate stage of the process (shown by the horizontal dashed lines) indicate *coherence* of the outgoing gluons: they are first produced in the form of specific gluomagnetic field configuration, the *turning states* at the figure above, which we study right now [60].

The top point is known as the *sphaleron*[15] configuration [55], first found in the context of electroweak theory. Intensive studies of the instanton-induced processes also were done in this context in early 1990's, driven basically by possible observability of baryon number violating processes in electroweak theory[33]. The so called "holy grail function" showed that processes with multiple quanta production indeed lead to growing cross section, reaching its maximum at the sphaleron mass and then decreasing. However,

[15]Which means "ready to fall" in Greek.

since in electroweak theory the maximal cross section has been found to be still very far from observability, the interest to this direction have mostly disappeared around 1993 or so.

At this second, Minkowski, stage the action is real, and the factor $exp(iS)$ does not affect the probability, and we only need to consider it for final state distributions. The sphaleron mass in QCD is

$$M_{sph} \approx \frac{30}{g^2(\rho)\rho} \sim 2.5\, GeV \tag{39}$$

Since those field configurations are close to classically unstable saddle point at the top of the barrier, they roll downhill and develop gluoelectric fields. When both become weak enough, solution can be decomposed into perturbative gluons. This part of the process can also be studied directly from classical Yang-Mills equation: for electroweak sphalerons it has been done in Refs[56], calculation for its QCD version is in progress [60]. While rolling, the configurations tend to forget the initial imperfections (such as a non-spherical shapes) since there is only one basic instability path downward: so the resulting fields should be nearly perfect spherical expanding shells. Electroweak sphalerons decay into approximately 51 W,Z,H quanta, of which only about 10% are Higgs bosons, which carry only 4% of energy. Ignoring those, one can estimate mean gluon multiplicity per sphaleron decay, by simple re-scaling of the coupling constants: the result gives 3-4 gluons. Although this number is not large, it is important to keep in mind that they appear as a coherent expanding shell of strong gluonic field.

In [59] we have tried to formulate a phenomenological model which would reasonably well describe describe data on various hadronic processes. In particular, we have shown that with the cross section of "sphaleron production" (per unit rapidity) by two "effective quarks" [16] being $\sigma_{qq} = 1.69 * 10^{-3} fm^2$, one can understand data about the energy growth of $NN, \pi N, \gamma N, \gamma\gamma$ cross sections. Furthermore, one can understand the effective power of the energy dependence versus impact parameter b, in pp collisions, see comparison in Fig. 14.

The next issue we address is whether the instanton approach can explain difference is the growing parts for different hadrons. To check that we need first to get the number of "relevant partons" for the nucleon, pion, and photon are summarized below in Table 1. The references given in the table are

[16] Those are defined as the number of quarks plus twice the number of gluons. Their number is evaluated from the structure functions. If integrated above the value of the Feynman $x \approx 0.01$ we get about 12 effective quarks/nucleon.

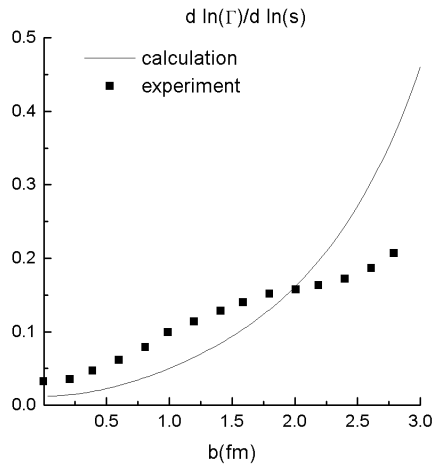

Figure 14: Effective power of the s-dependence of NN cross section, $\Delta(b)$, as a function of the impact parameter, b. Its decrease at small b is a consequence of "shadowing" of assumed instanton generated growing cross section by the ordinary color exchanges (with large but s-independent cross section). The squares marked "experiment" originate from the total and elastic amplitudes, those are taken from Kopeliovich et al. The line is our model. The agreement is not spectacular, but reasonable for a parameter-free model.

revised GRV parton distributions evaluated at next-to-leading order (NLO), taken at the scale of $Q^2 = 1$ GeV, which are then integrated over interval $x = [0.01, 1.0]$.

In principle, with more accurate parameterizations, we might try to test parton additivity by separately extracting, from the data of the *growing* part of hadronic cross section, the contributions of qq, qg, and gg to semi-hard processes. This was attempted, but with the accuracy at hand the differences between taking quarks and gluons is negligible. We are therefore forced to make a model-dependent assumption about their relative magnitude.

The instanton model [59] leads to a simple rule: changing a quark to a gluon result in extra Casimir factor 2. (It is different from the usual SU(3) Casimir scaling because we deal with SU(2) instanton fields, basically, although derivation is rather involved.) Therefore one can simply take the effective number of partons to be N_q+2N_g, where N_q and N_g are the numbers of quarks and gluons, respectively, taken from Table 1. This leaves us with only one unknown: the growing part of the qq cross section.

Combining the parton content with this simple recipe, one obtains the ratios of cross sections which may be compared to the coefficients of $\ln(s)$

Proton, with NLO structure functions GRV
$N_g = 4.10$
Valence $N_u = 1.70$
Valence $N_d = 0.84$
Sea $N_{u+d} = 1.16$
Pion, with NLO structure functions from GRV
$N_g = 3.1$
Valence $N_{u+\bar{d}} = 1.8$
Sea $N_{u+d} = 0.48$
Photon, with NLO structure functions from GRV
$N_g = 1.9\ \alpha$
$N_u = N_{\bar{u}} = 0.87\ \alpha$
$N_d = N_{\bar{d}} = 0.30\ \alpha$

Table 1: Partonic content of scattered particles (α is the fine structure constant).

extracted from experiment. The results, summarized in Table 2, are reasonable, but cannot be taken as precise since shadowing corrections have not been considered here.

Ratio	Computed	Part.Data Group
$\frac{1}{\alpha}\frac{X_{\gamma N}}{X_{NN}}$	0.50	0.43
$\frac{X_{\pi N}}{X_{NN}}$	0.73	0.63
$\frac{1}{\alpha}\frac{X_{\gamma\gamma}}{X_{\gamma N}}$	0.69	0.68

Table 2: Cross Section ratios as computed in the text and reported by the Particle Data Group.

After detailed study of shadowing in pp, we determined the quark-quark cross section to be $\sigma_{qq} = 1.69 \times 10^{-3}$ fm^2. We are now able to calculate the rising parts of total cross sections for other hadrons, and our precitions for $p\pi$, $p\gamma$, and $\gamma\gamma$ are given in Table 3. We find reasonable agreement between these numbers and the data, having fixed only one free parameter, c.

6.3 Instanton-induced production in heavy ion collisions

It has been suggested in [51] that if sphaleron-type object are copiously produced they may significantly increase the entropy produced and speed up

	Calculated	Part.Data Gr.
$X_{p\pi}$	0.132	0.111
$X_{p\gamma}$	5.65×10^{-4}	5.51×10^{-4}
$X_{\gamma\gamma}$	1.72×10^{-6}	1.45×10^{-6}

Table 3: Coefficients $X_{ij} = d\sigma_{ij}^{tot}/d\ln(s)$ in fm^2 for different hadronic constituents.

the equilibration process, as compared to mini-jet based scenarios considered previously.

For symmetric, central AA collisions of two nuclei we use the simplest model, one of two spheres with homogeneously distributed partons. The total parton number is AN_q, with $N_q \approx 12$ being the number of "effective quarks" (quarks number plus twice gluons number) per nucleon[17].

The total number of qq collisions in this case is easily obtained from the follwing geometric integral:

$$\begin{aligned} N_{coll} &= 8\pi\sigma_{qq}n_q^2 \int_0^R dr_t r_t \left(R^2 - rt^2\right) \\ &= 3^{4/3}2^{-5/3}\pi\sigma_{qq}n_q^2 \left(\frac{AN_q}{\pi n_q}\right)^{4/3}, \end{aligned} \tag{40}$$

where the quark density is determined by the nuclear density to be $n_q = N_q \times 0.16$ fm^{-3}.

With $A = 197$ (gold) and the value for the quark-quark cross section extracted above, $\sigma_{qq} = 1.69 \times 10^{-3}$ fm^2, we have the following production rate per unit rapidity of sphaleron-like clusters:

$$\frac{dN_{coll}}{dy} \approx 76.5\,, \tag{41}$$

a number somewhat smaller than estimated in Ref. [51].

Each cluster will in turn decay into a number of quarks and gluons. Simply scaling of the couplings from the studies of sphaleron decay in electroweak theory leads to about 3.5 gluons per cluster, with 0-6 quarks (up to a complete set of light quark-antiquark pairs, $\bar{u}u\bar{d}d\bar{s}s$). As an average we tentatively take 3.5 gluons and 2.5 quarks, the latter obtained by applying a factor of one half for the suppression of strange quarks and another one

[17]Of course, the clustering of partons into "constituent quarks" and nucleons increases the number of collisions, but we will ignore such correlations for now.

half to account for the possibly change in Chern-Simons number. This yields an average of six partons per cluster, or in central $AuAu$ collisions at RHIC about $76.5 \times 6 = 460$ partons per rapidity from sphaleron production. This is roughly *one half* the maximal possible value, $dN_{partons}/dy \sim dN_{hadrons}/dy \sim$ 1000, inferred experimentally from the final entropy limitations.

This result is in good agreement with phenomenological studies of the energy and impact-parameter dependence of multiplicity [57], which have deduced that the contribution to multiplicity which scales as the number of parton collisions generates about half of the total, when calculated from the standard Glauber model and using the experimental nuclear density distribution for a gold nucleus. In this picture, the ~ 500 hadrons per unit rapidity are then a result of prompt production from QCD sphalerons.

7 Brief Summary

In Lecture 1 we have discussed QCD vacuum, and concluded that the most important part of quark vacuum states are those with very small Dirac eigenvalues, made of *collectivized instanton zero modes*. Those form the quark condensate and in general dominate quark propagators at not-too-small distances.

In Lecture 2 we have studied the Euclidean correlation functions, the best bridge between theory, experiment and numerical experiment (lattice). Phenomenology of correlators is based on hadronic phenomenology, but is more directly related to quark motion and interaction. Dramatic instanton effects has been discussed, and some examples of truly quantitative description of (the tau decay) data has been shown. Again, keeping quasi-zero modes in all propagators does the job.

in Lecture 3 we learned that the QCD vacuum is not the only phase this theory may have. At least three directions are known, leading to quite different phases, and nearly all phase boundaries can be explained with instantons. At *high* T the instantons and anti-instantons form closed pairs with the top.charge zero: this restores chiral symmetry and lead to semi-perturbative phase known as *Quark-Gluon plasma*. At *high density* or chemical potentials, quark matter with intricate set of *Color superconducting phases* appear. In this case instantons and even one-gluon exchanges (at very high densities) create quark-quark Cooper pairs, which condense. Those play the role of composite Higgs scalar, and is in many respect similar to the Standard Model.

In Lecture 4 we discussed recent progress in heavy ion physics, devoted to experimental production of Quark-Gluon Plasma. New facility, RHIC, has just started, with many puzzling results. We have seen that its first data already show a spectacular explosion, driven by the predicted "QGP push". Many more puzzling phenomena, such as apparent jet disappearance in central collisions, are also discussed.

Lecture 5 was based on more recent material, it is attempts to explain old Pomeron phenomenology in terms of instanton-induced dynamics. The main lesson is that glue can be produced, from unphysical Euclidean paths to physical Minkowski evolution, in forms of the static magnetic "turning states", the relatives of the sphaleron. It was also conjectured that those objects are important for explaining RHIC data, and puzzling rapid production/equilibration of the QGP.

Acknowledgments. It is a pleasure to thank the organizers of the school, Alexei Smirnov and Goran Senjanovic, for their kind invitation and help during the school. It was indeed a very successful school, where people (I, at least) have learned a lot. This work was supported in parts by the US-DOE grant DE-FG-88ER40388.

References

[1] E.V. Shuryak, "The QCD Vacuum, Hadrons and the Superdense Matter," *SINGAPORE, WORLD SCIENTIFIC (1988) 401p*

[2] T. Schafer and E.V. Shuryak, Rev.Mod.Phys. 70 323 1998 hep-ph/9610451

[3] CHIRAL SYMMETRY BREAKING BY INSTANTONS. D. Diakonov, In *Varenna 1995, Selected topics in nonperturbative QCD* 397-432. e-Print Archive: hep-ph/9602375

[4] E.V. Shuryak, Rev. Mod. Phys. 651 1993

[5] M.A. Shifman, A.I. Vainshtein and V.I. Zakharov, Phys. Lett. 76B 471 1978

[6] E.V. Shuryak, Nucl. Phys. B203 93,116,140 1982

[7] V.A. Novikov, M.A. Shifman, A.I. Vainshtein and V.I. Zakharov, Nucl. Phys. B191 301 1981

[8] A.A. Belavin, A.M. Polyakov, A.S. Schvartz and Yu.S. Tyupkin, Phys. Lett. B59:85-87, 1975

[9] S.L. Adler, *Phys. Rev.*, 177:2426, 1969

[10] J.S. Bell and R. Jackiw, *Nuo. Cim.*, A60:47, 1969

[11] A. Hasenfratz and C. Nieter, Instanton Content of the SU(3) Vacuum, hep-lat/9806026

[12] G. 't Hooft, Phys. Rev. D14, 3432, 1976

[13] Y. Nambu and G. Jona-Lasinio, *Phys. Rev.* 122 345 1961

[14] D. Diakonov and V.Yu. Petrov, Nucl. Phys. B272:457, 1986

[15] M.A. Shifman, A.I. Vainshtein and V.I. Zakharov, Nucl. Phys. B165:45, 1980

[16] A. Blotz and E.V. Shuryak, Phys. Rev. D55:4055-4065, 1997

[17] R. Barate *et al.*, [ALEPH Collaboration], Z. Phys. **C76**, 15 (1997)

[18] R. Barate *et al.*, [ALEPH Collaboration], Eur. Phys. J. **C4**, 409 (1998)

[19] T. Schäfer, E.V. Shuryak, and J.J.M. Verbaarschot, Nucl. Phys. B412 143 1994

[20] R. Rapp, T. Schäfer, E.V. Shuryak and M. Velkovsky, Phys. Rev. Lett. 81 53 1998

[21] M. Alford, K. Rajagopal and F. Wilczek, Phys. Lett. B422 247 1998

[22] J.B. Kogut, M.A. Stephanov and D. Toublan, hep-ph/9906346

[23] R. Rapp, E.V. Shuryak and I. Zahed, Phys. Rev. D63:034008, 2001: hep-ph/0008207

[24] M. Alford, J. Bowers and K. Rajagopal, Phys. Rev. D**63**, 074016, 2001, [hep-ph/0008208]

[25] C. Gattringer, M. Gockeler, C.B. Lang, P.E. Rakow and A. Schafer, hep-lat/0108001; T. DeGrand, hep-lat/0106001; T. Blum *et al.*, hep-lat/0105006; R.G. Edwards and U.M. Heller, hep-lat/0105004; I. Hip, T. Lippert, H. Neff, K. Schilling and W. Schroers, hep-lat/0105001; T. DeGrand and A. Hasenfratz, hep-lat/0103002

[26] S. Hands, I. Montvay, M. Oevers, L. Scorzato and J. Skullerud, Nucl. Phys. Proc. Suppl. **94**, 461, 2001, [hep-lat/0010085]

[27] Proceedings of Quark Matter 2001, Stony Brook Jan. 2001, Nucl. Phys. A, in press

[28] E.V. Shuryak and I. Zahed, hep-ph/0005152; Phys. Rev. D, in press

[29] M. Nowak, E.V. Shuryak and I. Zahed, Soft Pomeron from Interacting Instantons, in progress

[30] D. Kharzeev and E. Levin, BNL-NT-99-8, Dec 1999, 12pp. hep-ph/991221

[31] E. Shuryak, `hep-ph 0001189`

[32] D. Kharzeev, Y. Kovchegov and E. Levin, hep-ph/0007182

[33] A. Ringwald, Nucl. Phys. B330 (1990) 1; O. Espinosa, Nucl. Phys. B343 (1990) 310; V.V. Khoze, A. Ringwald, Phys. Lett. B259:106-112, 1991; V.I. Zakharov, Nucl. Phys. B353 (1991) 683; M. Maggiore and M. Shifman, Phys. Rev. D46:3550-3564, 1992

[34] D.T. Son, Phys.Rev. D59 094019 1999; hep-ph/9812287

[35] D.T. Son, M.A. Stephanov and A.R. Zhitnitsky, hep-ph/0103099

[36] D. Teaney and E.V. Shuryak, Phys. Rev. Lett. **83**, 4951 (1999); [nucl-th/9904006]

[37] K.H. Ackermann *et al.*, [STAR Collaboration], "Elliptic flow in Au + Au collisions at s(N N)**(1/2) = 130-GeV," nucl-ex/0009011

[38] E. Shuryak, Phys. Rep. **61** , 71 (1980); Phys. Lett. **78B**, 150 (1978); Sov. J. Nucl. Phys. **28**, 408 (1978)

[39] J.Y. Ollitrault, Phys. Rev. **D46**, 229 (1992); Phys. Rev. **D48**, 1132 (1993)

[40] F. Karsch, E. Laermann, A. Peikert, Phys. Lett. B478:447-455, 2000: hep-lat/0002003

[41] C.M. Hung and E. Shuryak, Phys. Rev. **C57**, 1891 (1998)

[42] P.F. Kolb, J. Sollfrank and U. Heinz, hep-ph/0006129

[43] D. Teaney, J. Lauret, and E.V. Shuryak, in progress

[44] E.V. Shuryak, Invited talk at 14th International Conference on Ultrarelativistic Nucleus-Nucleus Collisions (QM 99), Torino, Italy, 10-15 May 1999. Nucl. Phys. A661:119-129, 1999; hep-ph/9906443

[45] M. Bleicher and H. Stocker, hep-ph/0006147

[46] Xin-Nian Wang, Miklos Gyulassy, Phys. Rev. D44:3501-3516, 1991

[47] B.B. Back *et al.*, [PHOBOS Collaboration], Phys. Rev. Lett. **85**, 3100 (2000) [hep-ex/0007036]

[48] J.P. Blaizot and A.H. Mueller, Nucl. Phys. **B289**, 847 (1987) Kajantie, P.V. Landshoff and J. Lindfors, Phys. Rev. Lett. **59**, 2527 (1987)

[49] T.S. Biro, E. van Doorn, B. Muller, M.H. Thoma and X.N. Wang, Phys. Rev. C **48**, 1275 (1993) [nucl-th/9303004]; L. Xiong and E. Shuryak, Phys. Rev. C **49**, 2203 (1994) [hep-ph/9309333]; R. Baier, A.H. Mueller, D. Schiff and D.T. Son, hep-ph/0009237

[50] M. Gyulassy, I. Vitev and X.N. Wang, Phys. Rev. Lett. **86**, 2537 (2001) [nucl-th/0012092]

[51] E.V. Shuryak, Phys. Lett. B **515**, 359 (2001)

[52] R. Rapp and J. Wambach, "Vector mesons in medium and dileptons in heavy-ion collisions", nucl-th/0001014.

[53] E. Kuraev, L. Lipatov and V. Fadin, Sov. Phys. JETP **45** (1977) 199; I. Balitsky and L. Lipatov, Sov. J. Nucl. Phys. **28** (1978) 822; L. Lipatov, Sov. Phys. JETP **63** (1986) 904

[54] D. Kharzeev, Y. Kovchegov and E. Levin, `hep-ph/0007182`; E. Shuryak and I. Zahed, Phys. Rev. **D62** (2000) 085014, `hep-ph/0005152`; M.A. Nowak, E.V. Shuryak and I. Zahed, hep-ph/0012232; Phys. Rev. D, in press

[55] N. Manton, Phys. Rev. D28 (1983) 2019; F.R. Klinkhamer and N. Manton, Phys. Rev. D30 (1984) 2212

[56] J. Zadrozny, Phys. Lett. B **284**, 88 (1992); M. Hellmund and J. Kripfganz, Nucl. Phys. B **373**, 749 (1992)

[57] D. Kharzeev and M. Nardi, Phys. Lett. B **507**, 121 (2001)

[58] L.D. McLerran and R. Venugopalan, Phys. Rev. D **59**, 094002 (1999); [arXiv:hep-ph/9809427]. A. Krasnitz, Y. Nara and R. Venugopalan, Phys. Rev. Lett. **87**, 192302 (2001), [arXiv:hep-ph/0108092]

[59] G. Carter, D. Ostrovsky and E. Shuryak,Instanton-induced Semi-hard Parton Interactions and phenomenology of High Energy Hadron Collisions, hep-ph/0112036

[60] G. Carter, D. Ostrovsky and E. Shuryak, in preparation